Numerical modelling of a voice-producing element

Monica Górska

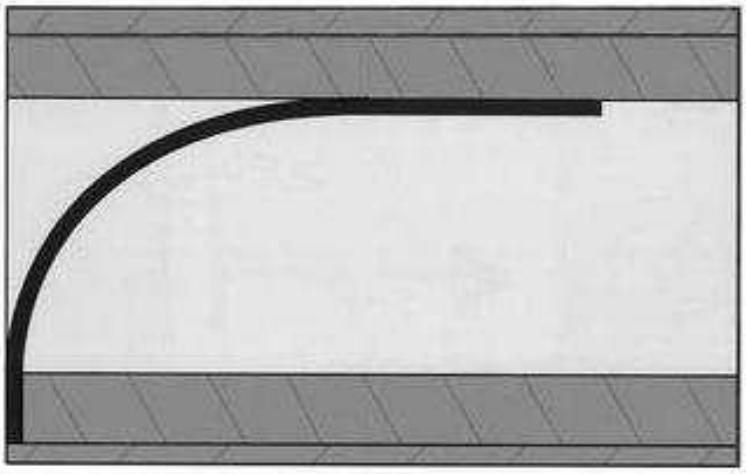

Department of
Mathematics

RuG

Master's Thesis

Numerical modelling of a voice-producing element

Monica Górska

Supervisor:
Prof.dr. A.E.P. Veldman
Department of Mathematics
University of Groningen
P.O. Box 800
9700 AV Groningen

December 2002

Contents

Introduction

During sound production at the larynx, air passes through the opening between the vocal folds, called the glottis, inducing the vocal folds to vibrate. This vibration of the vocal folds transforms the airflow into sound waves. Some patients with laryngeal cancer need a total laryngectomy to cure from the disease. In a total laryngectomy the vocal folds are removed (Figure 1). With this removal of the vocal folds, the natural way to produce voice is lost. A voice-producing element, which replaces the vocal folds, can be helpful. This voice-producing element consists of a single lip of silicone rubber in a cylindrical metal housing (Figure 2). This cylindrical metal housing has a square hole inside (Figure 3) and is placed in the shunt valve (Figure 4). The lip is fixed to the housing on one end. The other end is bent until it fits into the housing. This voice-producing element is already implemented in some patients, but there are a few disadvantages. For example, the intensity of sound with the voice-producing element is lower than the intensity in normal phonation.

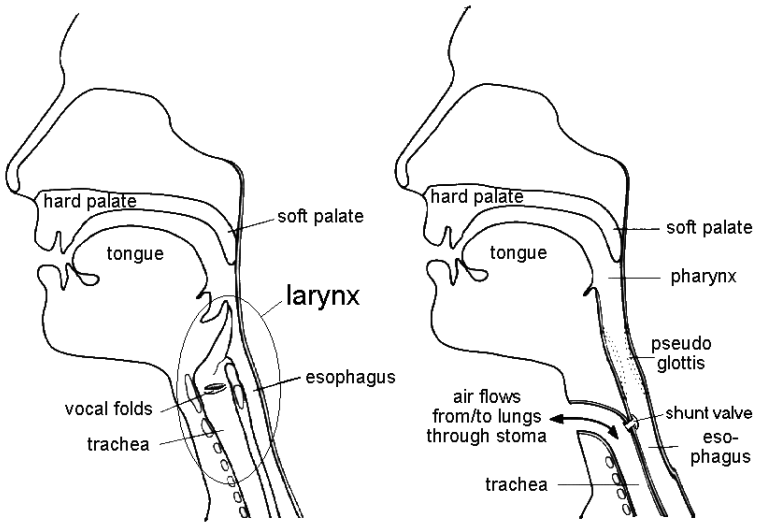

Figure 1: *Situation before (left) and after (right) laryngectomy.*

In designing an improved prototype for this voice-producing element, a numerical model can be useful. Up till now there are two different numerical models of the single lip of silicone rubber, the model of Hamburg [11] and the model of De Vries [29]. These two models will be discussed in this report. Also, a few aspects, like flow separation, initial load and leakage will be investigated, because these aspects raised some questions in the existing models. An overview of different models of vocal folds will be given first, before discussing the models of

the voice-producing element, to get more insight into the sound production.

This report consists of five chapters. An overview of different models of vocal folds will be given in chapter 1. In chapter 2 the mathematical and numerical model of the voice-producing element will be described. Numerical experiments and validation can be found, respectively, in chapter 3 and 4. Finally, the conclusions are presented in chapter 5.

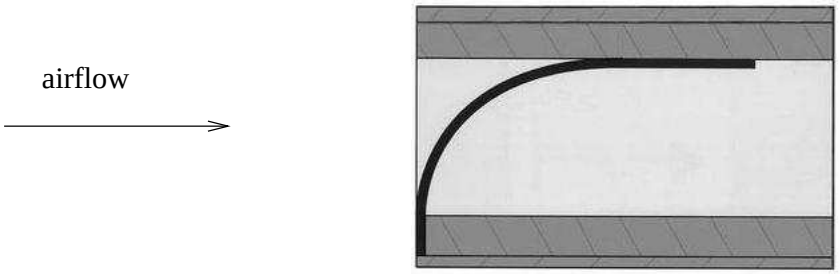

Figure 2: *Side view of the single lip in the housing (air flows from left to right).*

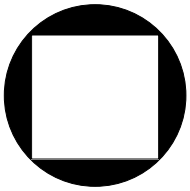

Figure 3: *Front view of the cylindrical metal housing with a square hole inside.*

Figure 4: *The shunt valve with inside the cylindrical metal housing.*

Chapter 1

Models of vocal folds

A numerical model can be useful to design an improved prototype for the voice-producing element. Before discussing the numerical models of the voice-producing element, an overview of different models of vocal folds [9] will be given in this chapter.

- One-mass model of Flanagan and Landgraf (1968)
- Two-mass model of Ishizaka and Flanagan (1972)
- Two-mass model of Pelorson (1994)
- Lumped parameter model of De Vries (2000)
- Three-mass model of Story and Titze (1995)
- 16-mass model of Titze (1973/1974)
- Finite-element model of Alipour and Titze (1988)

These models differ from each other by the number of parameters describing the vocal folds, by the value of the parameters or by the way aerodynamic influences are modelled. The two-mass models, the three-mass model and the finite-element model are the most familiar and the most used models. Therefore, these models are discussed in the following sections.

1.1 Two-mass models

In the two-mass model of Ishizaka and Flanagan [13], the vocal fold is divided in two parts, such that phase differences of the upper and lower parts are allowed. Each part consists of a simple mechanical oscillator having mass, spring and damper (Figure 1.1). The lower part of the vocal fold is made thicker than the upper part to include the effects of the body layer. This is because the body is found to be stiffer than the cover of the vocal fold. Ishizaka and Flanagan use the Bernoulli equation to model one-dimensional flow through the glottis. A few properties of the model are the fixed separation point at the end of the glottis, the abrupt closure of the glottis and the nonlinear behavior of the springs.

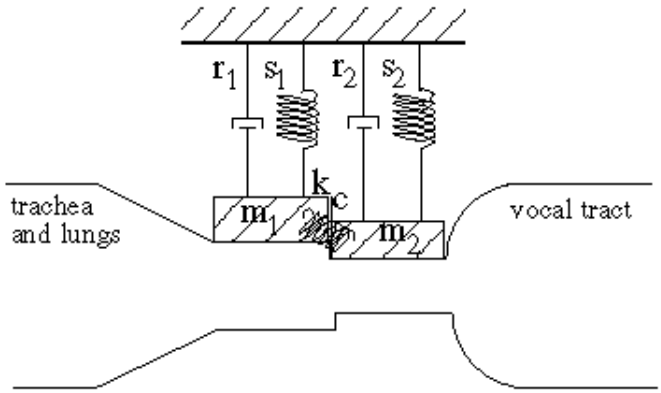

Figure 1.1: *The two-mass model of Ishizaka and Flanagan with mass m, spring s, damping r and coupling spring Kc.*

Another two-mass model is the one described by Pelorson [15, 16], who uses a different description of the aerodynamics. For example, Pelorson's model has a moving separation point within the glottis, the closure of the glottis occurs gradually and the behavior of the springs is linear. More differences between the model of Pelorson and the model of Ishizaka and Flanagan are given in Górska [9].

The collisions in both models are elastic. When the vocal folds touch each other, collision springs with different stiffness and dampers with different damping ratios will be activated and have an influence on m_1 and m_2 in the opposite direction. Both two-mass models have their own realistic properties. Combining the advantages of both models will probably result in an improved model of the vocal folds.

1.2 Three-mass model

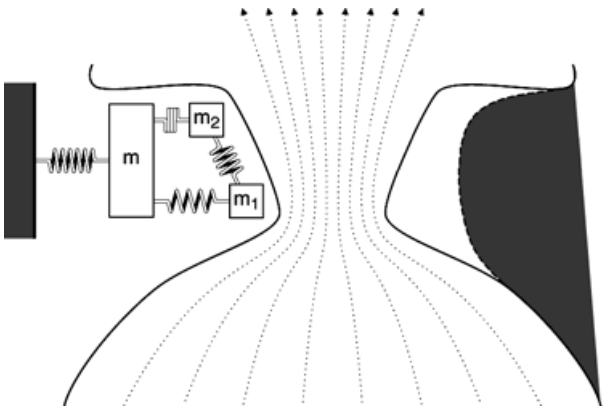

Figure 1.2: *The three-mass model of Story and Titze.*

In the three-mass model of Story and Titze [18] a distinction is made between body and cover of the vocal folds, because of different mechanical properties. This model (Figure 1.2) consists of two "cover" masses (m_1 and m_2), to keep the phase-difference like in the two-mass model, and one "body" mass (m). The body layer consists of muscle fibers and some tightly connected collagen fibers of the vocal ligament. The cover layer consists of pliable, non-contractile tissue. Simulations have shown similarity to observed vocal-fold motion, measured vertical phase difference, and mucosal wave velocity, as well as experimentally obtained intraglottal pressure. Unfortunately, no comparison with the two-mass models has been made.

1.3 Finite-element model

Alipour and Titze [1] used the finite-element method to study the physiology of phonation. This finite-element model (Figure 1.3) represents the geometry and the visco-elastic properties of the vocal folds accurately by dividing up the domain into small elements. Because these researchers do not compare the obtained results with results from normal phonation, their results are not always convincing. De Vries [28], on the other hand, used the finite-element method to obtain realistic values for the parameters of the two-mass models and showed that these values produce glottal waves within normal ranges of phonation. He also discussed the modelling of the voice-producing element and chose the finite-element model for describing this element. This finite-element model of the voice-producing element will be discussed in the next chapter.

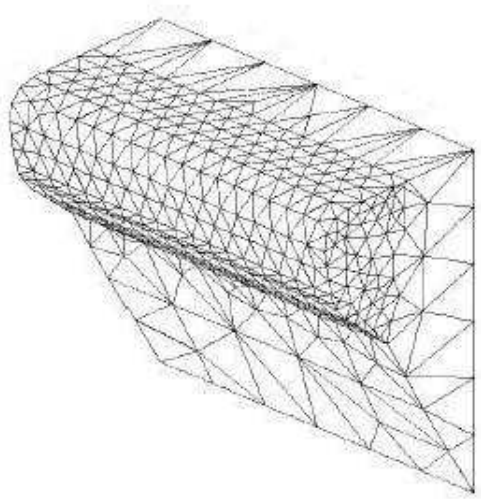

Figure 1.3: *The finite-element model of one vocal fold: the vocal fold is divided into small elements.*

Chapter 2

Simulation model of voice-producing element

This chapter describes both the mathematical model and the numerical model of the voice-producing element. In succession: the finite-element model of the lip, the aerodynamic part, the interaction between lip and air, the collision between lip and lower wall, and the determination of sound pressure level and spectrum will be described.

2.1 Finite-element model of the lip 2D

Mechanics

Using a finite-element model, the lip will be divided in several elements, connected to each other in nodes. In this report the lip consists of six elements and consequently it has seven nodes (Figure 2.1). Each element has three degrees of freedom at each node: horizontal displacement u in the x-direction, vertical displacement v in the y-direction and rotation ϕ.

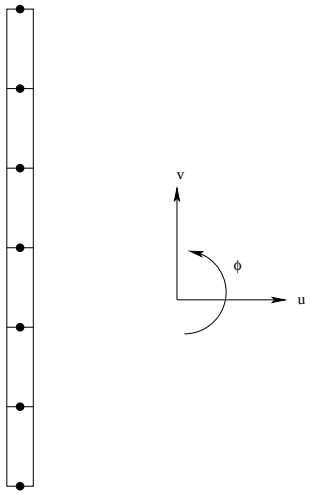

Figure 2.1: *The lip (in an upright position) consists of 6 elements and consequently it has 7 nodes.*

In the numerical model of the voice-producing element only displacements, velocities and accelerations due to bending will be considered. The lip is defined in an upright position first and then the lip is bent until it fits into the housing. A system of equations is constructed to describe the displacements and rotations with regard to the bending position of the lip:

$$[M^{sys}] \cdot \ddot{V}^{sys} + [C^{sys}] \cdot \dot{V}^{sys} + [K^{sys}] \cdot V^{sys} = Q^{q,sys} + Q^{\sigma,sys} \tag{2.1}$$

with $[M^{sys}]$ the mass matrix, $[C^{sys}]$ the damping matrix, $[K^{sys}]$ the stiffness matrix and V^{sys} the vector containing displacements and rotations of the nodes. Furthermore, the lip is subjected to a pressure generated by the lungs. The pressure that results from the airflow is translated into a distributed force and is stored in the vector $Q^{q,sys}$ and the forces acting on the lip as a result of the initial loads are stored in the vector $Q^{\sigma,sys}$. These initial loads are a result of the large deflection of the lip, because the lip has to fit into the housing.

Boundary Conditions

This system of equations requires boundary conditions. Because the lip is clamped on one end, the conditions are at the base of the lip:

$$\begin{gathered} \text{horizontal displacement } u_0 = 0 \\ \text{vertical displacement } v_0 = 0 \\ \text{rotation } \phi_0 = 0 \end{gathered}$$

and also the velocities and accelerations at the base of the lip have to be zero.

The system of equations will be solved with the Newmark-β method. For a detailed description of this method and the construction of the element mass, stiffness and damping matrices, see Hamburg [11].

Differences between the existing models

Two different models of the lip exist, one is made by Hamburg [11] and the other by De Vries [29]. The two main differences between these models, the determination of the damping matrix and the setting of the initial load, will be described below. The model of De Vries is still under development, and no definite results can be presented at the moment.

Determination of the damping matrix

Hamburg uses $[C] = \alpha[M] + \beta[K]$ with $\alpha = 85.9\ s^{-1}$ and $\beta = 8.0 \cdot 10^{-4}\ s$ to determine the damping matrix. These α and β are material parameters and can not be determined easily. Unfortunately, these values are not explained in his report.

De Vries, on the other hand, uses another relationship to determine the damping matrix, namely $[C] = 2\xi\sqrt{M \cdot K}$ with ξ is the damping factor, varying between 0 and 1 (1 is critically damped). In his simulations a damping factor $\xi = 0.025$ is used. Experiments have been done to determine this damping factor [29]. In the experiments the silicone rubber has been stretched and then released to derive this damping factor by looking at the damping behaviour. These experiments have been done only for very low frequencies (0 - 10 Hz),

whereas the frequencies from the simulations are much higher (200 - 300 Hz). This makes the value $\xi = 0.025$ uncertain.

Setting of the initial load

In both models, the lip is defined in an upright position first. Then the lip is bent in such a way that it rests against the housing of the voice-producing element. The model of Hamburg applies a force and a moment on the last node of the lip in such a way that the nodal coordinates will define the lip in its bending position against the housing. The calculation of the acting force and moment is carried out as a preprocessing step (using the ANSYS package).

As an alternative for bending the lip, in the model of De Vries a force along the entire length of the lip is applied. In his model an equally small perpendicular force is applied in each node, except the first one, to bend the lip. This small perpendicular force is increased until the lip fits into the housing; this determines the initial load $Q^{\sigma,sys}$. Moments are not considered in the nodes.

2.2 Aerodynamics

Navier-Stokes equations

To obtain oscillations of the lip, aerodynamic forces have to act on the nodes of the lip. In this report, the incompressible two-dimensional Navier-Stokes equations are used to determine these aerodynamic forces. The incompressible two-dimensional Navier-Stokes equations are as follows:

- Conservation of mass
$$\nabla \cdot \mathbf{u} = 0 \tag{2.2}$$
with $\mathbf{u} = (u, v)$ the velocity vector.

- Conservation of momentum
$$\frac{\partial \mathbf{u}}{\partial t} + (\mathbf{u} \cdot \nabla)\mathbf{u} = -\nabla p + \nu(\nabla \cdot \nabla)\mathbf{u} + \mathbf{F} \tag{2.3}$$
where p is the pressure, ν is the kinematic viscosity and $\mathbf{F}$ is the vector representing external forces on the air.

These equations require boundary conditions.

Boundary Conditions

Boundary conditions are needed at the voice-producing element's housing, at the inlet and at the outlet. At the voice-producing element's housing, the tangential velocity

$$\mathbf{u} \cdot \mathbf{t} = 0$$

(the no-slip condition) has to be satisfied, simulating the sticking of the air to the housing. Furthermore, the perpendicular velocity has to be zero

$$\mathbf{u} \cdot \mathbf{n} = 0,$$

simulating the impermeability of the housing.

At the inlet, the pressure has to be prescribed over the entire cross-section. The outlet conditions combine a prescribed pressure with zero normal derivatives of the velocities over the entire cross-section.

2.3 Interaction

There has to be continuity of pressure and velocity. In each time step the pressure distribution and air velocities are being calculated first. The pressure in air is being translated into aerodynamic forces that act on the element nodes. In return, the displacements and velocities of the lip are calculated and used as boundary conditions for the aerodynamic model (Figure 2.2).

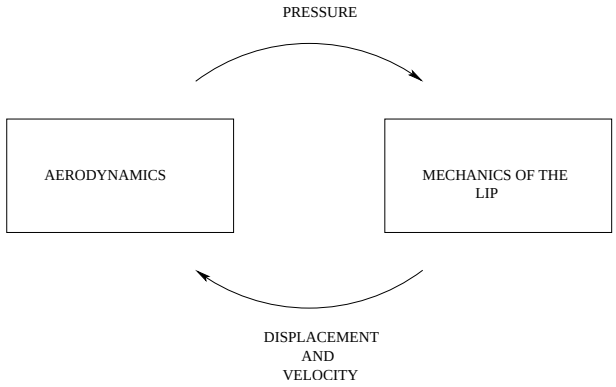

Figure 2.2: *Interaction between the aerodynamics and the mechanics of the lip.*

In this section a short survey will be given. During the interaction two types of coordinate systems are active, a global and a local coordinate system. The global coordinate system is defined in the grid and the local coordinate system is attached to an element. During the interaction with air, forces and velocities will be translated from the global coordinate system to the local coordinate system, using a rotation matrix. A more detailed description can be found in Hamburg [11].

The pressure of the adjacent air-filled grid cell is used to calculate the force in global coordinates that is applied by the air to the lip by multiplying the pressure with the area it acts on. This global force can be a horizontal force (F_x) that acts on the left and right surfaces of an element and/or a vertical force (F_y) that acts on the top and bottom surfaces of an element. These global forces are translated to local forces and then multiplied by a vector that contains functions by which the displacements and forces are distributed along the element. So far, the forces in the nodes are calculated and only have to be rotated back to the global coordinate system, since equation (2.1) is formulated in terms of the global coordinate system. At the end, the magnitude and direction of the forces that act on the different nodes

are known and stored in the vector $Q^{q,sys}$.

Now equation (2.1) can be solved to find the position of the lip at the new time level. The resulting velocities in the nodes (nodal velocities) of the lip are rotated from the global coordinate system to the local coordinate system. These nodal velocities in the local coordinate system are multiplied by a vector that contains functions by which the displacements and forces are distributed along the element. The velocities on the elements (local velocities) have been calculated then. Finally, these local velocities are rotated back to the global coordinate system and then simply assigned to the boundaries of the cells adjacent to the lip, acting as a boundary condition for the aerodynamic model.

2.4 Collision between lip and lower wall

The incompressible Navier-Stokes equations are used to describe the aerodynamics. When the lip makes contact with the lower wall, the air underneath the lip will be enclosed. If the lip moves in such a way such that the volume beneath the lip changes, it will be inconsistent with the assumed incompressibility of air. In more mathematical terms, the Poisson equation which has to be solved to compute the pressure does no longer have a solution. This problem is solved in the models by always keeping a little opening between the lip and the lower wall. This means the lip does not make contact with the lower wall and that is a disadvantage of the models. Another possibility to solve this problem is making a small pipe behind the base of the lip, allowing the air beneath the lip to escape (Figure 2.3). This solution does not need a little opening between the lip and the lower wall anymore, because the air will not be enclosed. Another possibility to prevent the enclosure of air is making a pipe before the base of the lip (Figure 2.4). The advantage of these solutions is that it allows collision between the lip and the lower wall.

Figure 2.3: *A pipe is created in the model of Hamburg to prevent the enclosure of air.*

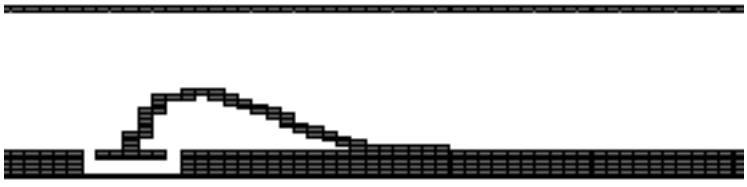

Figure 2.4: *Another pipe is created in the model of Hamburg to prevent the enclosure of air.*

In reality, leakage of air along the lip takes place on both sides of the lip. In three dimensions a small opening of about 0.2 mm exists at each side of the lip to prevent the lip to be fixed between the side walls. This leakage was not modelled in the numerical models of the lip, because these models are two-dimensional. However, leakage along the sides of the lip is modelled, when a pipe is introduced in the models.

2.5 Sound pressure level and spectrum

It is important that the sound produced by the voice-producing element resembles the sound from the vocal folds. Therefore, the sound pressure level and the fundamental frequency has to fall within physiologic ranges:

- The sound pressure level at comfortable effort should lie between 70 and 80 dB, measured at a distance of 30 cm from the mouth.
- The voice-producing element should have a fundamental frequency of about 110 Hz for males and about 210 Hz for females.
- The fundamental frequency of the sound should be varied between about -10% and 30% of the values, mentioned above, when the pressure difference across the element changes. This avoids monotonous speech.

The calculation of the sound pressure level and of the fundamental frequency will be discussed here.

Sound Pressure Level

In the literature, the sound pressure level (SPL) has only been calculated from measurements. A formula exists to calculate the SPL [24]:

$$SPL = 20Log(\frac{P}{P_0}) = 10Log(\frac{P}{P_0})^2, \tag{2.4}$$

where P is the pressure and P_0 is the standard reference pressure of $2.0 \cdot 10^{-5}\ Pa$. Unfortunately, this formula can not be used directly, because pressure is a function of time. The Bernoulli equation

$$p(t) + \frac{1}{2}\rho q(t)^2 = c(t) \tag{2.5}$$

can be helpful, where $p(t)$ is the pressure, ρ is the density, $q(t)$ is the velocity and $c(t)$ is a function which is constant along streamlines. The Bernoulli equation expresses the conservation of fluid energy. The air which flows through the inlet has to flow with the same amount through the outlet after some time. First, the Bernoulli equation has to be integrated over the cross-section. Second, the pressure can be divided into a mean pressure and a deviation of the mean pressure. This gives the following equation:

$$\begin{aligned}[\int\int p\,\mathrm{d}y\mathrm{d}z]_{mean} + \delta[\int\int p\,\mathrm{d}y\mathrm{d}z] + \frac{1}{2}\rho([\int\int q^2\,\mathrm{d}y\mathrm{d}z]_{mean} + \delta[\int\int q^2\,\mathrm{d}y\mathrm{d}z]) \\ = [\int\int p\,\mathrm{d}y\mathrm{d}z]_{mean} + \frac{1}{2}\rho[\int\int q^2\,\mathrm{d}y\mathrm{d}z]_{mean},\end{aligned} \tag{2.6}$$

where z is the direction perpendicular on the xy-plane, from (2.6) follows:

$$\delta[\int\int p\,\mathrm{d}y\mathrm{d}z] = -\delta[\int\int q^2\,\mathrm{d}y\mathrm{d}z]. \tag{2.7}$$

The term $\int\int q^2\,\mathrm{d}y\mathrm{d}z$ has been calculated in the program. The SPL can be calculated by determining the standard deviation of $\int\int q^2\,\mathrm{d}y\mathrm{d}z$ first and after that using the formula (2.4). A corresponding matlab-file can be found in the appendix.

Spectrum

Spectrums can be calculated with Fourier analysis. The Fourier transform decomposes or separates a waveform into sinusoids of different frequency which sum to the original waveform. The Fourier transform $F(s)$ of a signal $f(t)$ is defined as:

$$F(s) = \int_{t1}^{t2} f(t)e^{-i2\pi ts}\,\mathrm{d}t. \tag{2.8}$$

In our situation the signal $f(t)$ is the flux $\int\int q\,\mathrm{d}y\mathrm{d}z$ and has also been calculated in the program. A corresponding matlab-file can be found in the appendix.

Chapter 3

Numerical sensitivity experiments

In the simulations the lip has been modelled using the dimensions for the voice-producing element that was used during the in vitro experiments. This lip is called prototype 11 and has the following dimensions:

Length lip : 8.5 mm,
Width lip : 5 mm,
Thickness lip : 0.25 mm.

In this chapter, the following aspects have been investigated: flow separation, initial load and leakage. This research is done, because these aspects raised some questions in the model of Hamburg [11]. First, a preliminary validation of the model of Hamburg will be given.

3.1 Preliminary Validation

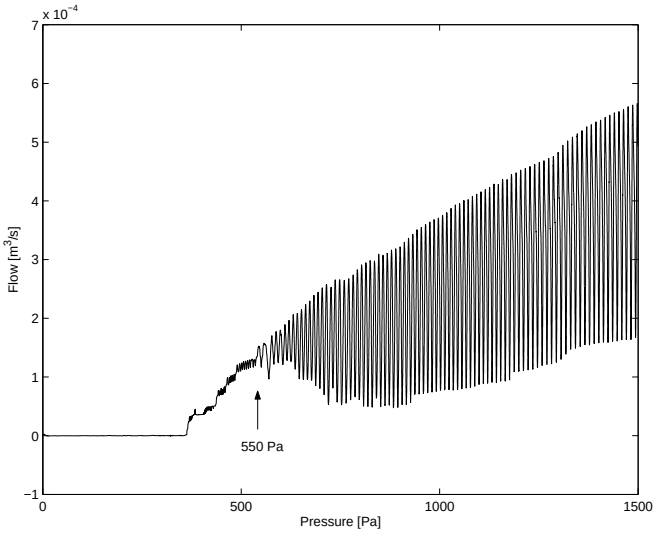

Figure 3.1: *Model of Hamburg when the prescribed pressure is increased from 0 Pa to 1500 Pa.*

The pressure in normal phonation varies between 0 Pa (silence) and 3000 Pa (screaming). The phonation threshold pressure is the smallest pressure in the subglottal area (trachea) at which self-sustained oscillation of the vocal folds begins. Below this phonation threshold pressure, damped oscillation occurs. Theoretical calculations of the threshold pressure range between 200 and 400 Pa [8, 23, 25, 27]. A simulation of the model of Hamburg has been performed for prototype 11, beginning with a pressure of 0 Pa up to 1500 Pa (Figure 3.1). Looking at Figure 3.1, the phonation threshold pressure is about 550 Pa which is larger than the theoretical phonation threshold pressure, but acceptable. Besides that, one can see a horizontal line in the beginning of the simulation. This horizontal line is realistic, because the air pressure is not high enough in the beginning to exceed the initial load. The lip still rests against the upper wall and therefore no flow of air appears.

3.2 Flow Separation

When air flows along the lip, flow separation occurs. A flow separation point is the point where the flow is detached from the lip. It depends on the position of the lip if the flow separation point is situated at the end of the lip (Figure 3.2) or somewhere else on the lip (Figure 3.3 and 3.4). This flow separation point has not been calculated directly in the program, but follows from the calculation in the model. The position of a separation point is important, because it has an influence on the flow. The question is how accurate the position of the separation point is. Therefore, grid refinement has been performed to investigate this accuracy. The grid (horizontal x vertical) is varied in both directions for 800 and 2000 Pa. Simulations have been performed for three different grids, 100 x 30, 150 x 50 and 200 x 60 (Table 3.1). The simulations for 2000 Pa with grid 150 x 50 and 200 x 60 has been broken down, because the end of the lip is bent backwards and the model does not allow this. The cause of this bending is probably the unrealistic initial load at the end of the lip. Simulations without applying the moment did not break down.

	100 x 30	150 x 50	200 x 60
Mean Flow [L/s]	0.178	0.20	0.20
Frequency [Hz]	277	295	295
SPL [dB]	68.7	68.8	68.9

Table 3.1: *Results of numerical simulations for different grid (800 Pa).*

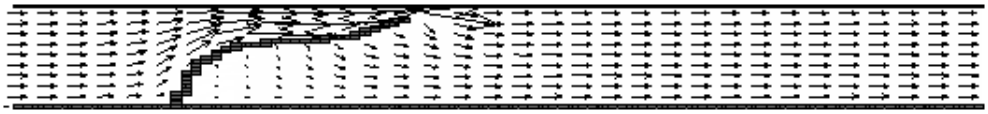

Figure 3.2: *Flow is detaching at the end of the lip.*

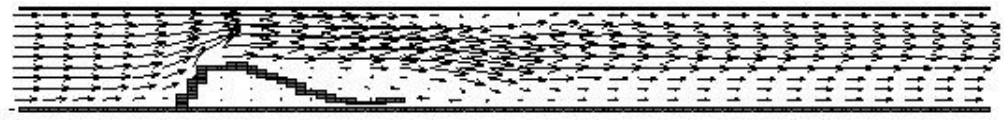

Figure 3.3: *Flow is detaching somewhere else on the lip.*

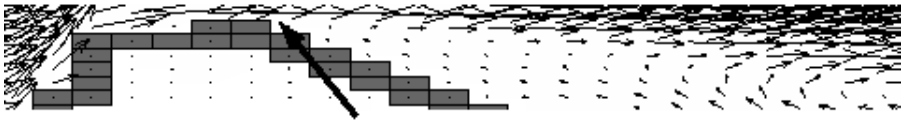

Figure 3.4: *Flow is detaching where the arrow is pointing at (zoomed picture).*

Comparing the results in the simulations with different grid mesh, the flow separation point seems to be at the same place for the same position of the lip. If the position of the lip is like the position in Figure 3.2, then the flow separation point will be at the end of the lip. If the position of the lip is like the position in Figure 3.3, then the flow separation point will be at the position where the lip is mostly bent (Figure 3.5 and 3.6). Although the separation point is in the same position for the same position of the lip for all grids, the grids 150 x 50 and 200 x 60 for a pressure of 800 Pa show other values for flow, frequency and sound pressure level than the 100 x 30 grid (Table 3.1). The grid 200 x 60 gives the same results as the grid 150 x 50. Simulations should be performed with the 150 x 50 grid, because these results are more accurate than the results from the 100 x 30 grid. However, the 100 x 30 grid is still preferred, because the finer grid gives problems for simulations with 2000 Pa, i.e. the backwards bending of the end of the lip.

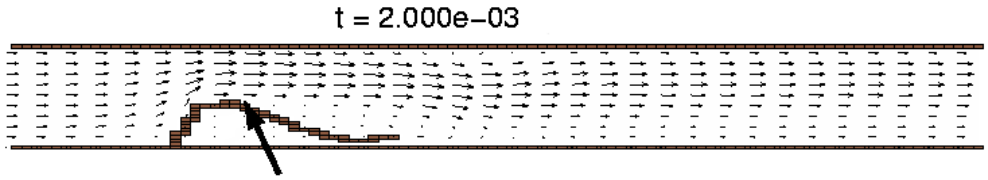

Figure 3.5: *The flow separation point is situated where the arrow is pointing at* (100 x 30).

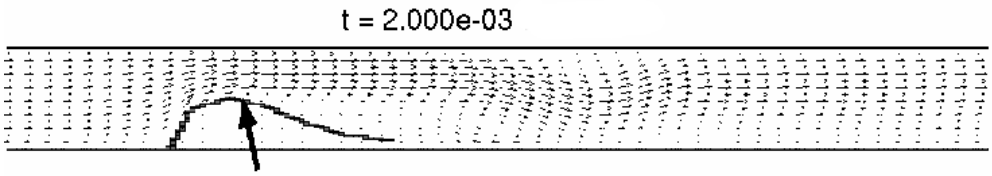

Figure 3.6: *The flow separation point is situated where the arrow is pointing at* (200 x 60).

Hamburg [11] has also varied the grid mesh and showed that the mean flow of the 150 x 50

grid did not differ from the mean flow of the 100 x 30 grid (Table 3.2) in contrast with the results in Table 3.1. An explanation can be found in using different parameter values in the inputfiles or in the accuracy of determining the mean flow.

	100 x 30	150 x 50
Mean Flow [L/s]	0.19	0.19
Frequency [Hz]	272	303

Table 3.2: *Results of numerical simulations of Hamburg (800 Pa).*

3.3 Initial Load

The initial load in the model of Hamburg is a force and a moment at the end of the lip. Unfortunately, this moment at the end of the lip causes an unrealistic upwards bending of the end of the lip (Figure 3.7). De Vries is currently working on a model where the initial load, which only consists of forces, is distributed over the entire lip [29].

Figure 3.7: *Upwards bending of the end of the lip.*

Reducing Initial Load

The calculated initial load (by ANSYS) on the last node is a force $F_y \approx 0.38 \cdot 10^{-2}\ N$ and a moment $M_z \approx 0.51 \cdot 10^{-5}$. Simulations with these values are performed at two different pressures, 800 and 2000 Pa. Also, simulations have been carried out with an initial load (force and moment) which is made 2 and 4 times smaller to get more insight in the influence of the initial load. The results of the simulations are shown in Table 3.3 and 3.4 and also presented in the Figures 3.8 - 3.13. These figures consists of two graphics. The first one is the flow as function of time and the second one is the frequency spectrum, where the height of a frequency is related to the sound pressure level. This relation should follow from Fourier Analysis, which is used to determine the frequency spectrum. In lowering the initial load, the following conclusions can be made:

- the mean flow gets smaller,
- the fundamental frequency gets lower,
- the sound pressure level gets lower,
- the amplitude of the flow gets smaller,

- the peak of the fundamental frequency in a FFT spectrum gets smaller,
- and the slope between the first and second peak in a FFT spectrum gets less steep.

Furthermore, the initial load appears to be very important to get a good movement of the lip. If there is no initial load, the lip will hardly move. Making the initial load too small, for example 8 times smaller than the calculated initial load ($F_y \approx 0.04 \cdot 10^{-2} N$, $M_z \approx 0.06 \cdot 10^{-5}$), the flow will hardly oscillate (Figure 3.14). When making the initial load too large, for example 2 times larger than the calculated initial load ($F_y \approx 0.76 \cdot 10^{-2} N$, $M_z \approx 1.02 \cdot 10^{-5}$), the end of the lip will bend backwards and because the model does not allow this, the simulation breaks down.

	calculated initial load	2 times smaller	4 times smaller
Mean Flow [L/s]	0.178	0.154	0.118
Frequency [Hz]	277	248	239
SPL [dB]	68.7	66.9	60.5

Table 3.3: *Results of numerical simulations for different initial loads (800 Pa).*

	calculated initial load	2 times smaller	4 times smaller
Mean Flow [L/s]	0.497	0.446	0.353
Frequency [Hz]	340	208	192
SPL [dB]	74.9	73.3	71.6

Table 3.4: *Results of numerical simulations for different initial loads (2000 Pa).*

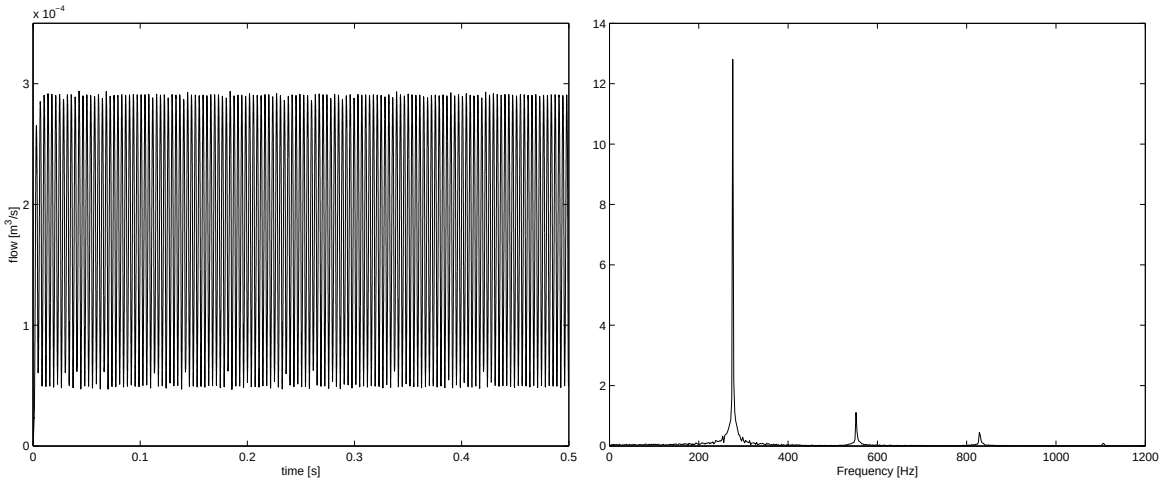

Figure 3.8: *Hamburg's model for 800 Pa with calculated initial load. Flow as a function of time (left) and the frequency spectrum (right).*

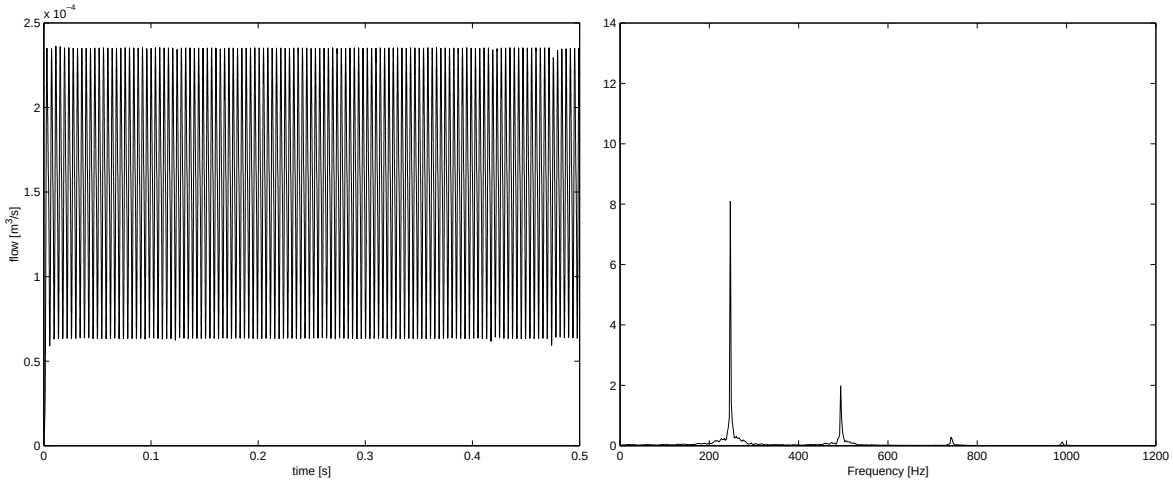

Figure 3.9: *Hamburg's model for 800 Pa with initial load 2 times smaller. Flow as a function of time (left) and the frequency spectrum (right).*

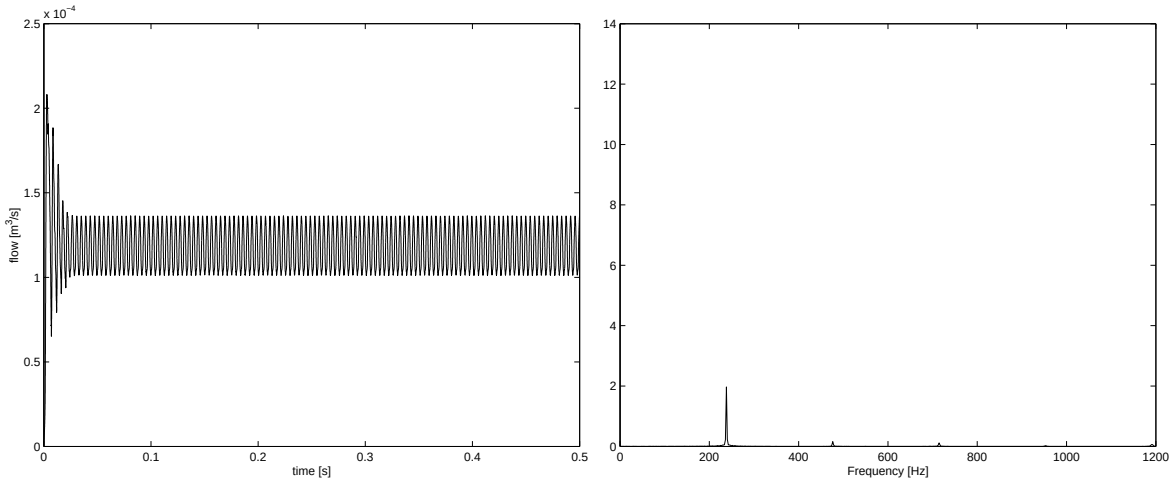

Figure 3.10: *Hamburg's model for 800 Pa with initial load 4 times smaller. Flow as a function of time (left) and the frequency spectrum (right).*

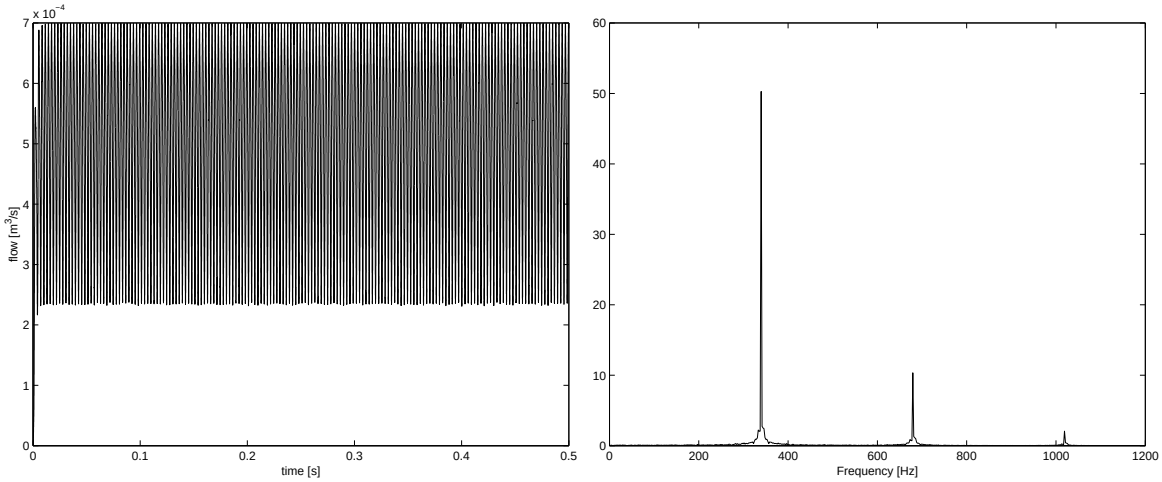

Figure 3.11: *Hamburg's model for 2000 Pa with calculated initial load. Flow as a function of time (left) and the frequency spectrum (right).*

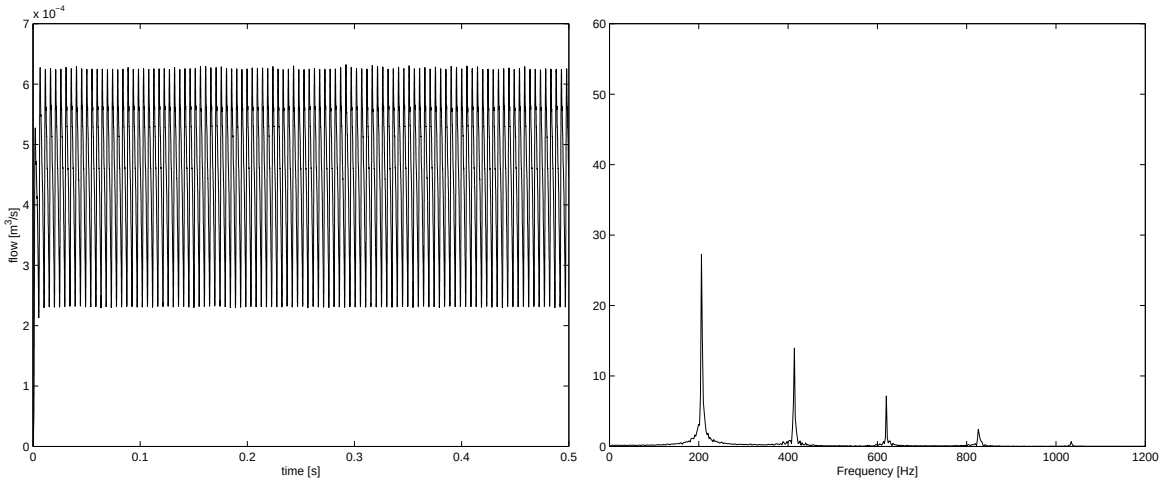

Figure 3.12: *Hamburg's model for 2000 Pa with initial load 2 times smaller. Flow as a function of time (left) and the frequency spectrum (right).*

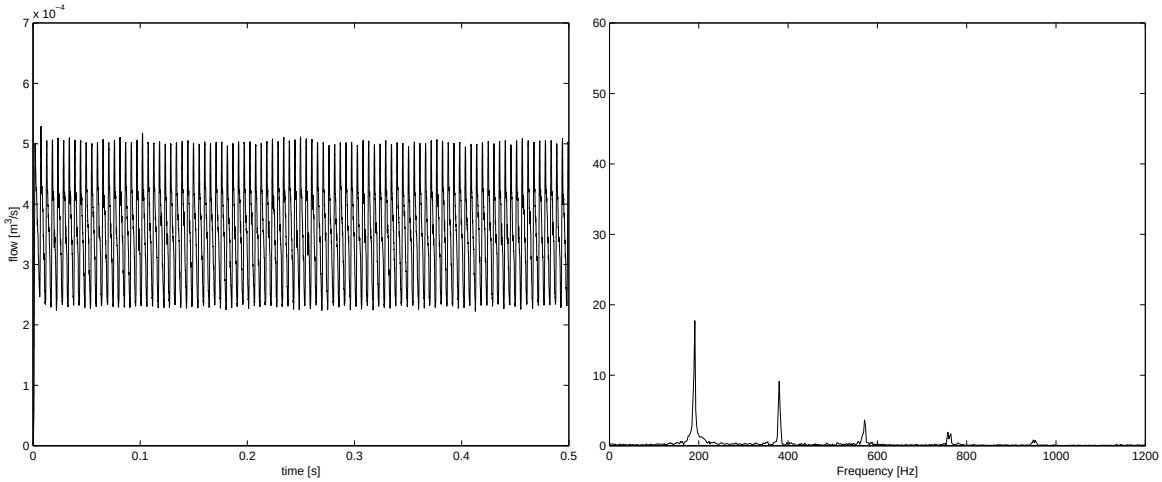

Figure 3.13: *Hamburg's model for 2000 Pa with initial load 4 times smaller. Flow as a function of time (left) and the frequency spectrum (right).*

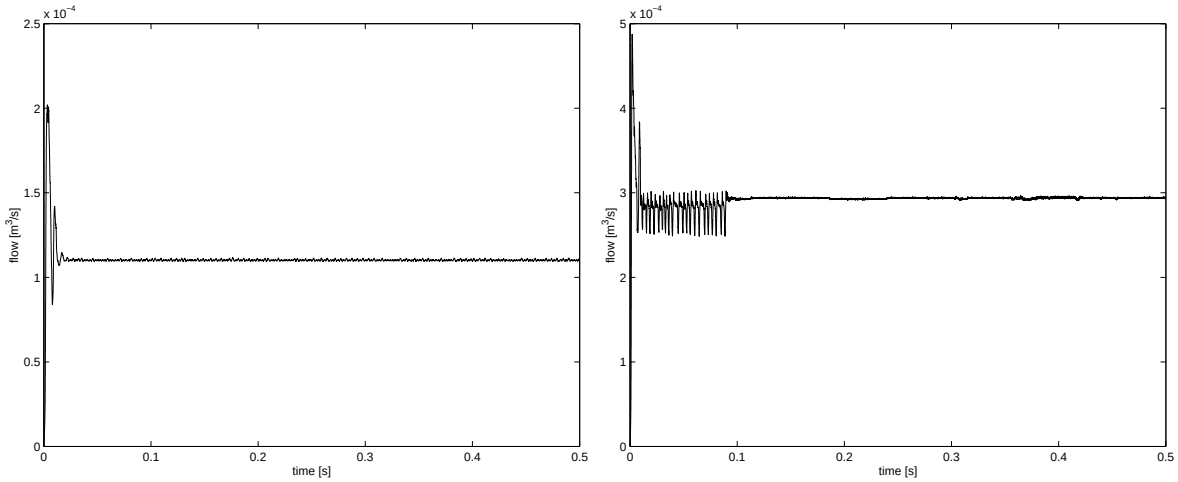

Figure 3.14: *Hamburg's model with initial load 8 times smaller. Flow as a function of time for 800 Pa (left) and 2000 Pa (right).*

3.4 Leakage

Simulations for high pressures and without keeping a small opening break down, when the lip collides with the lower wall. The same simulations with a pipe in the model did not break down. Two options exist for the position of a pipe: a pipe behind the base of the lip (Figure 3.15) and a pipe before the base of the lip (Figure 3.16). A pipe behind the base of the lip models leakage at the back of the lip. A pipe before the base of the lip models leakage in front of the lip.

Figure 3.15: *A pipe behind the base of the lip (pipe 1) is created in the model of Hamburg to prevent the enclosure of air.*

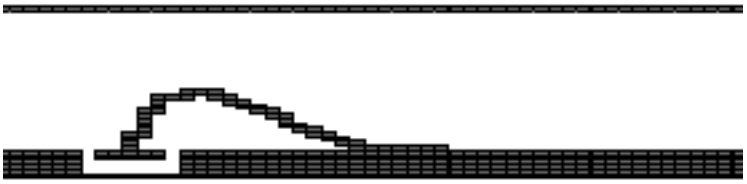

Figure 3.16: *A pipe before the base of the lip (pipe 2) is created in the model of Hamburg to prevent the enclosure of air in another way.*

Two simulations for 2000 Pa have been carried out to show the results of the different pipes in the model and to know how much air flows through these pipes (Table 3.5 and Figures 3.17 and 3.18). The diameter of the pipes is 0.3 mm. The simulation without a pipe but with a small opening between the lip and the lower wall is also shown in Table 3.5. The pressure of 2000 Pa is chosen, because then the lip makes contact with the lower wall (in case of the simulations with a pipe) and the pipes become important to avoid enclosed air. When a pressure of 800 Pa is applied, the lip did not come near the lower wall. Simulations with both pipes are also carried out, but these results will be presented later.

The results from the model with pipe 1 are almost simular to the results from the model without a pipe. On the contrary, the results from the model with pipe 2 show much more difference when compared to the results from the model without a pipe. The mean flow is smaller and the fundamental frequency is higher in the model with pipe 2 when compared to the results from the model without a pipe. Another observation is that the mean flow in pipe 1 is very small, about 0.5% of its total mean flow and the mean flow in pipe 2 is about 10 % of its total mean flow.

	model without a pipe, but with a small opening	model with pipe 1	model with pipe 2
Mean Flow [L/s]	0.497	0.497	0.360
Frequency [Hz]	340	335	380
SPL [dB]	74.9	74.5	73.9
Mean Pipe Flow [L/s]	-	0.0026	0.035

Table 3.5: *Results of numerical simulations for model without and with a pipe (2000 Pa).*

From Figure 3.17, one can see the flow in pipe 1 is sometimes negative, which means air flows backwards in the pipe. This negative flow in pipe 1 was not expected, because this pipe was made in such a way that air underneath the lip could escape when the lip collides with the lower wall. Negative flow has not be seen in pipe 2 (Figure 3.18). Moreover, the flow in the pipes depends on the position of the lip. The maxima of the flow in pipe 1 correspond with a high position of the end of the lip. The minima of the flow in pipe 1 correspond with a very low position of the end of the lip (the lip collides with the lower wall). These results were not expected, because the leakage at the back of the lip is expected to be the largest when the lip (almost) collides with the lower wall, because then the air underneath the lip can 'only' escape through the pipe. In case of the flow in pipe 2 it is the same: maxima correspond with a high position and the minima with a low position of the end of the lip. These results were expected. The leakage is expected to be the largest when the lip (almost) collides with the upper wall, because in that case the airflow has 'no other' possibility to escape than through the pipe. Snapshots of the movement of the lip near the upper and lower wall can be found in the appendix.

The following conclusions can be made from these simulations:

- A pipe built in the model in such a way that it prevents enclosed air, allows collision between the lip and the lower wall.
- Two options exist for making a pipe in the model such that it prevents enclosed air: a pipe before the base of the lip and a pipe behind the base of the lip. Both are modelling leakage along the sides of the lip. A pipe before the base of the lip models leakage in front of the lip and a pipe behind the base of the lip models leakage at the back of the lip.
- Leakage in front of the lip appears to be larger than leakage at the back of the lip. Moreover, negative flow appears in the pipe behind the base of the lip. This negative flow does not appear in the pipe before the base of the lip.

In the following chapter, these results will be validated with the results from in vitro experiments.

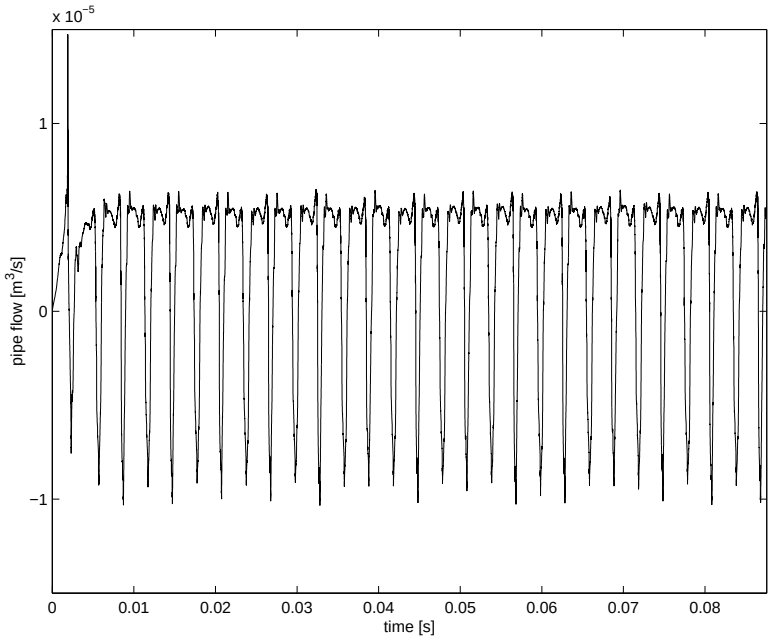

Figure 3.17: *Hamburg's model with pipe 1. The flow through the pipe for some period of time (mean flow* $0.497 \cdot 10^{-3}\ m^3/s$*).*

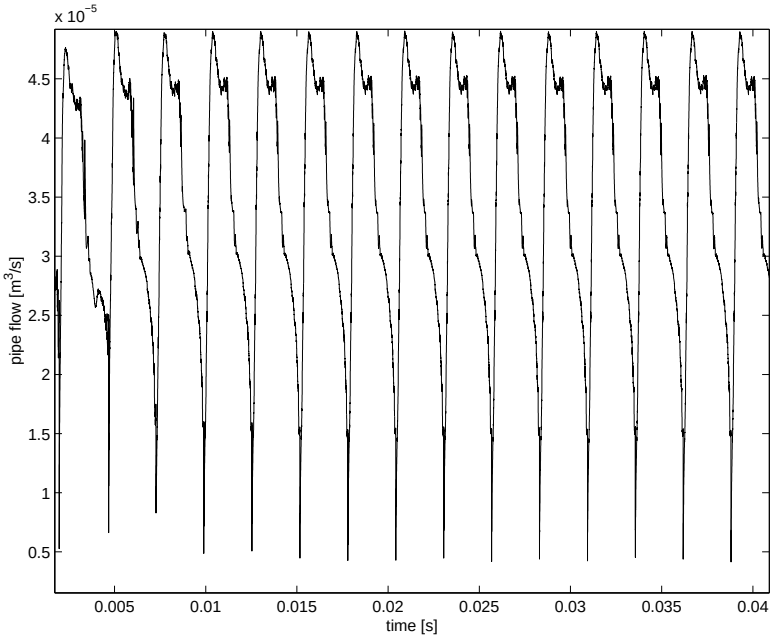

Figure 3.18: *Hamburg's model with pipe 2. The flow through the pipe for some period of time (mean flow* $0.360 \cdot 10^{-3}\ m^3/s$*).*

Finally, simulations have been performed with both pipes for 800 and 2000 Pa. The diameter of the pipes has been varied. The small pipes have a diameter of 0.3 mm and the larger pipes a diameter of 0.6 mm. The results of the simulations are shown in Table 3.6 and 3.7. The flow above the lip has also been calculated. Once again, the flow in pipe 2 is larger than the flow in pipe 1. When the diameter of the pipes is made two times larger, the flow in both pipes is also two times larger.

	model without pipes but with a small opening	model with 2 pipes of 0.3 mm	model with 2 pipes of 0.6 mm
Mean Flow [L/s]	0.178	0.199	0.200
Frequency [Hz]	277	285	275
SPL [dB]	68.7	68.8	68.0
Flow Pipe 1 [L/s]	-	-0.0007	-0.004
Flow Pipe 2 [L/s]	-	0.024	0.047
Flow above lip [L/s]	0.178	0.176	0.153

Table 3.6: *Results of numerical simulations for model without and with pipes (800 Pa).*

	model without pipes but with a small opening	model with 2 pipes of 0.3 mm	model with 2 pipes of 0.6 mm
Mean Flow [L/s]	0.497	0.433	0.400
Frequency [Hz]	340	375	365
SPL [dB]	74.9	74.6	74.1
Flow Pipe 1 [L/s]	-	0.005	0.011
Flow Pipe 2 [L/s]	-	0.037	0.072
Flow above lip [L/s]	0.497	0.396	0.328

Table 3.7: *Results of numerical simulations for model without and with pipes (2000 Pa).*

Chapter 4

Validation

In this chapter the results from simulations described in chapter 3 will be validated with in vitro experiments. These in vitro experiments have been performed by Van der Plaats [17]. The complete set-up for measuring the voice-producing element in vitro is described in De Vries [28]. First, simulations with the model of Hamburg without pipes have been carried out and validated with the in vitro experiments. And second, simulations with the model of Hamburg with one pipe (the pipe before the base of the lip and the pipe behind the base of the lip) have been performed and validated. The dimensions of the lip have already been given in chapter 3 and the dimensions of the housing are as follows:

Length housing : 9 mm,
Width housing : 5 mm,
Height housing : 3 mm.

These in vitro experiments have been performed with the shunt valve (Figure 4.1), which has been placed between a physical subglottal tract model (lungs and trachea) and a physical vocal tract model (pharynx, oral and nasal cavities). The results of these in vitro experiments for prototype 11 are shown in Table 4.1. In Table 4.2 the simulation results are given. Both results are also presented in Figure 4.2 and 4.3.

Figure 4.1: *The shunt valve with inside the cylindrical metal housing.*

Data of the sound pressure level (SPL) of this particular prototype of the in vitro experiments has not been found in literature. In normal phonation the SPL should lie between 70 and 80 dB, measured at a distance of 30 cm from the mouth [28]. The obtained values of the SPL in

Pressure [Pa]	780	1170	1370	2150	2350	2540	2740
Mean Flow [L/s]	0.13	0.18	0.25	0.29	0.32	0.36	0.4
Frequency [Hz]	253	231	221	231	243	253	275

Table 4.1: *In vitro results for prototype 11 including the shunt valve.*

Pressure [Pa]	780	1170	1370	2150	2350	2540	2740
Mean Flow [L/s]	0.174	0.291	0.369	0.523	0.559	0.617	-
Frequency [Hz]	275	266	260	345	360	380	-
SPL [dB]	68.5	71.2	72.6	75.2	75.5	76.6	-

Table 4.2: *The simulation results for prototype 11.*

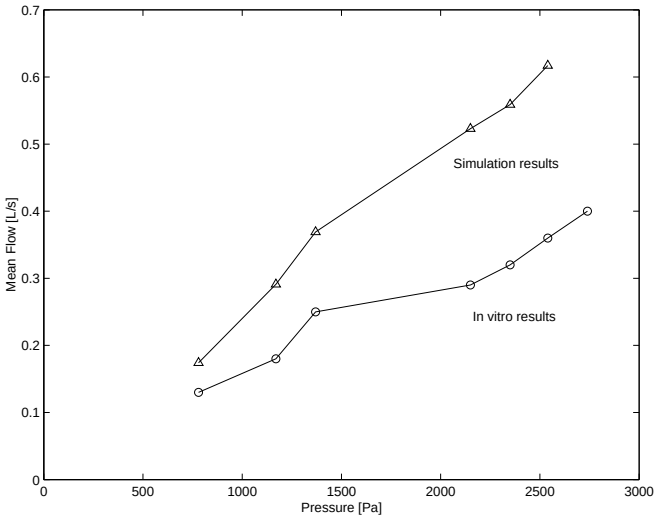

Figure 4.2: *Mean flow obtained from the numerical simulations and the in vitro experiments.*

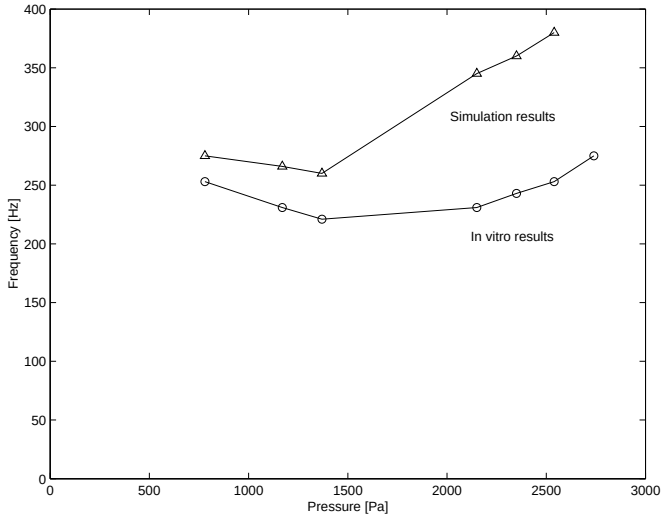

Figure 4.3: *Frequencies obtained from the numerical simulations and the in vitro experiments.*

the simulations are between 65 and 80 dB, but these values will be lower when the air flows through the vocal tract and 30 cm outside the mouth.

From Table 4.1, Table 4.2 and Figure 4.2, one can see the mean flow increases as the pressure rises. Furthermore, the mean flow of the simulation is larger than the mean flow of the in vitro experiment. From Figure 4.3, the fundamental frequencies obtained from the numerical simulations are also larger than the fundamental frequencies obtained from the in vitro experiments. Remarkable is the dip in the frequency curve in both numerical simulations and in vitro experiments. According to De Vries [28], the dip could be related to a change in vibration mode. Before this dip, the frequency decreases as the pressure increases, which is not desirable because this is not found in normal phonation. De Vries also investigated the influence of the shunt valve and showed that experiments without a shunt valve lead to a larger flow and a higher fundamental frequency. This leads to simulation results closer to in vitro results. These larger flow and higher fundamental frequency of the in vitro results without shunt valve are caused by a lower airflow resistance, because the airflow resistance of the voice-producing element is mainly influenced by the shunt valve [26, 28]. In vitro experiments with the lip in the housing, but without subglottal tract, vocal tract and shunt valve, could be done to make a better comparison between the simulation and in vitro results.

Although a better comparison can be made between the simulations and the in vitro experiments by changing the in vitro experiments as described above, there exist also a few drawbacks in the numerical model of Hamburg. In reality torsion of the lip, leakage along the sides of the lip and collision between the lip and the lower wall exist. These three aspects are all missing in the numerical model. Two of these aspects can be solved by making a pipe in the model (shown in section 2.4) such that collision between the lip and the lower wall can take place and simultaneously this pipe will model leakage. Simulations with the model with one pipe are performed and the results can be found in Table 4.3 and 4.4 and also in Figure 4.4 and 4.5.

Pressure [Pa]	780	1170	1370	2150	2350	2540	2740
Mean Flow [L/s]	0.169	0.291	0.358	0.533	0.572	-	-
Frequency [Hz]	266	267	260	345	356	-	-
SPL [dB]	68.1	71.2	72.2	75.0	75.5	-	-

Table 4.3: *The simulation results with a pipe behind the base of the lip (pipe 1) for prototype 11.*

Pressure [Pa]	780	1170	1370	2150	2350	2540	2740
Mean Flow [L/s]	0.194	0.288	0.307	0.377	-	-	-
Frequency [Hz]	280	292	302	393	-	-	-
SPL [dB]	68.8	71.1	72.0	74.2	-	-	-

Table 4.4: *The simulation results with a pipe before the base of the lip (pipe 2) for prototype 11.*

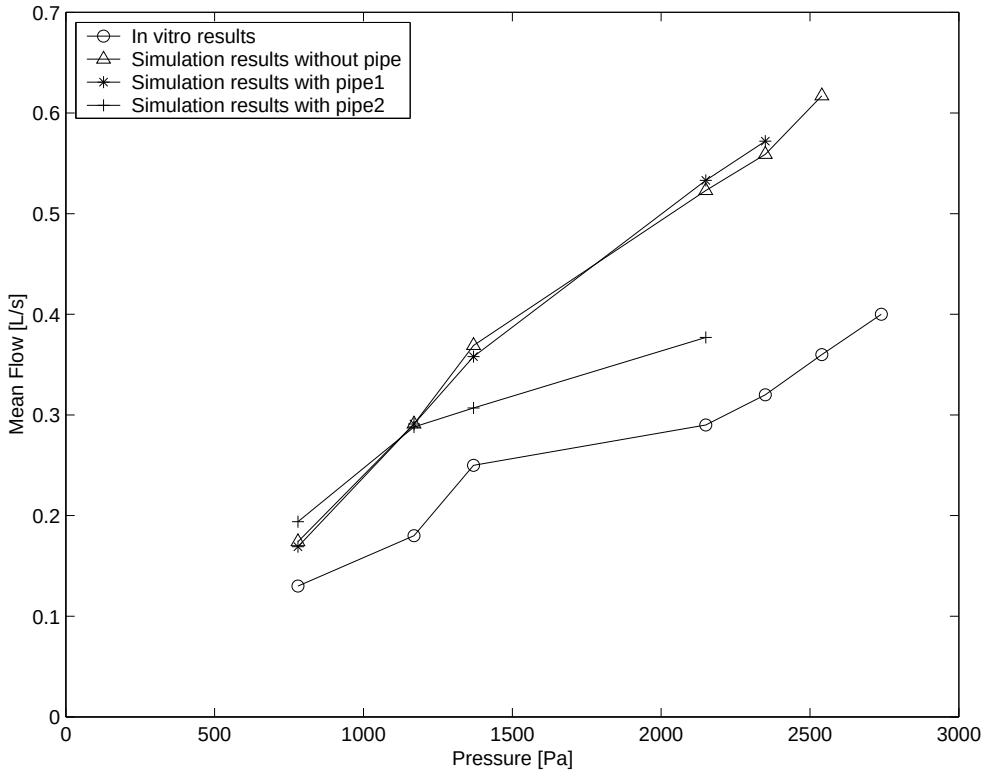

Figure 4.4: *Mean flow obtained from the numerical simulations and the in vitro experiments.*

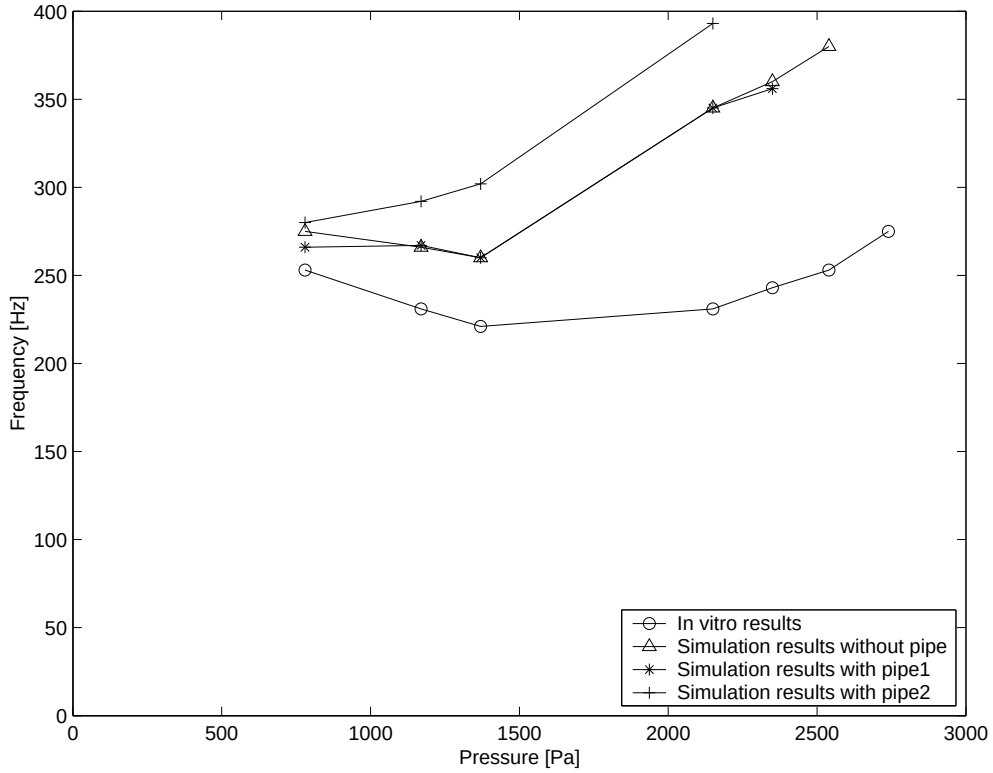

Figure 4.5: *Frequencies obtained from the numerical simulations and the in vitro experiments.*

The results from the simulations with pipe 1 are almost the same as the results from the simulations without pipe. However, the simulations with pipe 2 show different results. The mean flows of these simulations are closer to the mean flows of the in vitro experiments. These closer values may indicate that leakage in front of the lip is important to include in the numerical model. On the other hand, the differences in frequencies between the simulations with pipe 2 and the in vitro experiments are larger than the differences in frequencies between the simulations without pipe and the in vitro experiments. An explanation for this is not found. Sometimes, the numerical simulations for higher pressures broke down because of the backwards bending of the lip, which is probably caused by the unrealistic initial load at the end of the lip.

More research should be done to find a pipe such that it models leakage more realistic. For example, the diameter of the pipe and the position of the pipe could be varied. Otherwise, one should make a three-dimensional model to avoid this problem, because a three-dimensional model models leakage directly.

Chapter 5

Conclusions

In the model of Hamburg [11] some questions raised on three different aspects: flow separation, initial load and leakage. These aspects were investigated in this report.

The first one, flow separation, raised the question whether the position of the flow separation point is accurate. This question can be answered positive. In the simulations with varying grids, the flow separation point is in the same position for the same position of the lip. If the position of the lip is like the position as in Figure 5.1, then the flow separation point will be at the end of the lip. If the position of the lip is like the position as in Figure 5.2, then the flow separation point will be at the position where the lip is mostly bent.

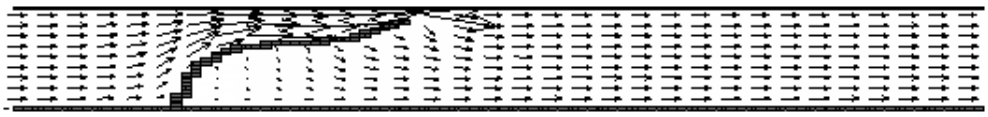

Figure 5.1: *Flow is detaching at the end of the lip.*

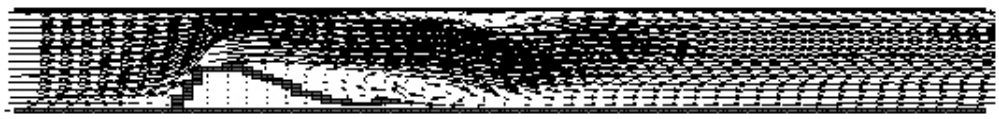

Figure 5.2: *Flow is detaching where the lip is mostly bent.*

The second aspect, the initial load, appears to be important to obtain good movement of the lip. Although an initial load of a force and a moment only at the end of the lip in the model of Hamburg is less realistic than an initial load of forces distributed over the entire lip in the model of De Vries, the model of Hamburg is still the only working model. Because the initial load appears to be very important, more research is needed to find the proper initial load.

The last aspect, leakage, is investigated because it was not modelled in the model of Hamburg. Moreover, in his model no collision takes place between the lip and the lower wall, because a small opening is made to prevent enclosed air beneath the lip. If the lip moves such that the

volume beneath the lip changes, it will be inconsistent with the assumed incompressibility of air. Another way to avoid inclusion of air is applied in this report by making a pipe before or behind the base of the lip (Figure 5.3 and 5.4). These pipes have two advantages:

- a small opening between the lip and the lower wall is not needed anymore and therefore collision can take place between the lip and the lower wall;
- a pipe models leakage along the sides of the lip that in reality exists.

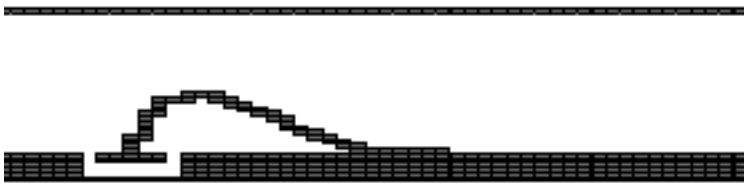

Figure 5.3: *A pipe before the base of the lip is created in the model of Hamburg to prevent the enclosure of air.*

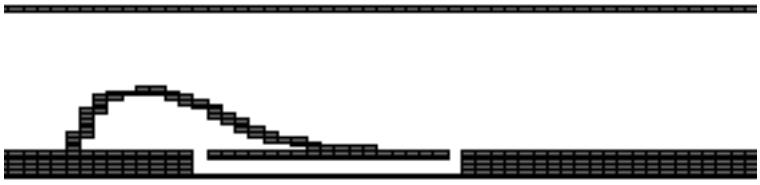

Figure 5.4: *A pipe behind the base of the lip is created in the model of Hamburg to prevent the enclosure of air.*

The results from the simulations with a pipe at the back of the lip are almost the same as the results from the simulations without pipe. The simulations with a pipe in front of the lip show different results. The mean flows in these simulations are closer to the mean flows of the in vitro experiments. These closer values may indicate that leakage in front of the lip is important to include in the numerical model. On the other hand, the differences in frequencies between the simulations with a pipe in front of the lip and the in vitro experiments are larger than the differences in frequencies between the simulations without pipe and the in vitro experiments. An explanation for this has not been found.

Recommendations

The results of the numerical model show many differences with the in vitro measurements, but some improvements are possible to get closer results between the numerical model and the in vitro experiments.

Firstly, in vitro experiments can be performed with only the lip in the housing, without subglottal tract, vocal tract and shunt valve, because the simulations are also performed without subglottal tract, vocal tract and shunt valve. This enables a better comparison between the simulation and the in vitro results.

Secondly, more research is needed to find the proper initial load, because this appears to be very important for the movement of the lip. De Vries is currently working on a model where the initial load, which only consists of forces, is distributed over the entire lip [29].

Finally, more research can be done to find a pipe such that it models leakage more realistic. As an alternative, the model can be made three-dimensional to model the leakage directly. An additional advantage of modelling the lip three-dimensional is allowing torsion of the lip.

Appendix A

Program Description

The numerical model has been implemented in a FORTRAN program: HEAT97. In this appendix, information is given about the calling sequence in section A.1 and about the subroutines in section A.2.

A.1 Calling Sequence

```
Initialisation    SETPAR   GRID
                  SETFLD   LDMECH
                           MCHLBL

Time cycle loop   INIT     BCBND    MCHOBS
                           MCHOBS
                  TILDE    BDYFRC
                  SOLVEP   COEFF
                           MILU
                           BCBND    MCHOBS
                  CFLCHK   DTADJ
                  MCHPF
                  MCHFOLD  MKSYSTEM
                           TMANUF
                           REDUCE
                           SOLVE
                           BACK_T
                           COLLIDE
                  MCHLBL
```

A.2 Subroutines

In this section a short description of the subroutines is given.

BACK_T : determines the new coordinates of the lip.
BCBND : sets boundary conditions for velocity components.
BDYFRC : computes the apparent body force.

CFLCHK	:	monitors the CFL-number and sets flag for time-step adjustment.
COEFF	:	defines coefficient matrix for Poisson equation, including boundary conditions at the wall and at the obstacle.
COLLIDE	:	keeps the lip between the housing.
DTADJ	:	halves/doubles time step (old time step will be repeated).
GRID	:	makes a (non-uniform) grid.
INIT	:	starts a new time step.
LDMECH	:	reads the inputfiles mech.in and bendflap.txt, bends the lip into the housing.
MCHFOLD	:	calls the following subroutines: mksystem, tmanuf, reduce, solve, back_t, collide.
MCHOBS	:	determines the velocities around the lip.
MCHLBL	:	produces rotation matrices and labels the lip elements.
MCHPF	:	translates the air pressure into nodal forces.
MILU	:	solves the Poisson equation.
MKSYSTEM	:	produces system matrices.
PRT	:	prints and writes results.
REDUCE	:	adds the transformation matrices to the system matrices.
SETFLD	:	initializes the fluid configuration.
SETPAR	:	reads the inputfile heat97.in.
SOLVE	:	applies the Newmark-β method to calculate the resulting displacements, velocities and accelerations at each node.
SOLVEP	:	organizes the pressure calculation and updates the velocity.
TILDE	:	integrates the momentum equations.
TMANUF	:	produces element transformation matrices to reduce the degrees of freedom (the axial strain will be made zero).

Appendix B

Input Files

This program needs three inputfiles, called **bendflap.txt**, **heat97.in** and **mech.in**. The inputfile **bendflap.txt** is created by ANSYS and is given below.

```
NODE      UX
   1   0.0000
   2  0.37214E-03
   3  0.13518E-02
   4  0.26567E-02
   5  0.40639E-02
   6  0.54800E-02
   7  0.68955E-02

NODE      UY
   1   0.0000
   2 -0.50254E-04
   3 -0.44405E-03
   4 -0.13096E-02
   5 -0.25625E-02
   6 -0.40246E-02
   7 -0.55000E-02

NODE      ROTZ
   1   0.0000
   2 -0.52579
   3 -0.98602
   4  -1.3351
   5  -1.5519
   6  -1.6307
   7  -1.5708

NODE      FY
   7 -0.38676E-02
```

```
    NODE      MZ
       7  0.51040E-05
```

The vectors UX, UY and ROTZ consists of respectively horizontal displacements, vertical displacements and rotations for each node that lies on the lip; FY and MZ consists of respectively a force and a moment acting at the free end of the lip.

The inputfiles **heat97.in** and **mech.in** are listed below. The following settings in these files were used as input for the simulation of prototype 11 (see chapter 3).

```
***** tank geometry ************************************************
icyl     Xmin      Xmax     Ymin     Ymax        spec.geom.
  0      0.0       0.03     0.0      0.003        2

***** grid definition *********************************************
iMaxUs   jMaxUs    cx    cy     xpos    ypos
 100       30      0     0      0.025   0.004

***** liquid properties *******************************************
 Nu      IHeat  Pran   Rayl(-g*beta)   rho   c_p
1.33e-5       0    0.71    0.0         1.2   1

**** gordijnparameters ********************************************
Vgordyn  Tgordyn  Tbinnen  Tbuiten  Tvloer (<0 = adiabat.)
  4.0      35.0     20.0      5.0   -15.0

***** body forces and external motion: 2D **************************
Gx      TxOn    TxOff    u0       Gy    TyOn    TyOff    v0
0.0     0.0      100    0.0      0.0    0.0    100.0   0.0
Ampl    Freq    Angle
0.0     0.0      0.0
Rpm     DelOme  TwUp    TwDown      x0     y0
0.0      0.0     0.0      10.0      0.0    0.0

***** body forces and external motion: axisymmetric ****************
  Gy    TyOn    TyOff   v0     Ampl    Freq
 0.0    0.0      100   0.0     0.0     0.0
 Rpm    DelOme  TwUp    TwDown
 0.0     0.0    5.0      17

***** boundary conditions and inflow characteristics ***************
left    right   top   bottom   UIn    VIn   Freqin    IPIn  PIn
 7        7      2       2     0.0    0.0    0.0      1     2000
```

```
***** upwind parameter and Poisson iteration parameters *************
Alpha       Epsi       ItMax   OmStrt   IMilu
1.0       1.0e-8        500      1.3       0

***** time step and restart control *********************************
TFin      DelT     CFLMax   PrtDt     svst   svdt
0.5       1e-6      0.5    1.0e-2       0     10.0

***** print/plot control ********************************************
gnu      avs   uvpt   velop   forces
 0        0      1      0       0

***** stream lines **************************************************
nrx   nry   nrdt   xps     yps     xqs     yqs      t   dt/delt
  0     0      0   40.0   30.0    80.0    63.0    0.1     1

***** fluxes ********************************************************
number of fluxes to be printed (flux01.out...flux##.out are created)
    0
   p1     p2     p3     hor   (explanation below)

***** PD ************************************************************
number of PD to be printed (PD01.out...PD##.out are created)
  0
sigma
  50
 x      y
```

The file **mech.in** has the following structure:

```
c Length       Width    Height     E         Density     Number of Elm.   afdrukref
  8.50E-3    5.0E-3  0.25E-3    8.6E6     1.13E3          6                 1
c
c
c
c
c
c
c  orig        delta     dampcoeff    Refvalue     T_Jump
   5.0E-3      0.51      2.0           0.0         1.0e-5
c  Cmass     Cstiff
   85.9      8.0e-4
```

Another inputfile **heat97.geo** is needed to make one or two pipes in the model. Such a file is given below. Two pipes of 0.3 mm are implemented.

```
Icyl   Xmin    Xmax    Ymin    Ymax
  0     0.0    0.03    -0.0005   0.003
arcs          line segment  inflow     outflow
    0            5           0           2
arcs:
  xm     ym       r   teta1   teta2  side  left  right  up  under  m.points
line segments:
  x1        y1       x2    y2   kant  left  right   up  under  m.points
  0.0040 -0.0005  0.0040  0.0    0     1      0      0     0      0
  0.0135 -0.0005  0.0135  0.0    1     0      1      0     0      0
  0.0043 -0.0002  0.0058  0.0    2     0      0      0     0      0
  0.0061 -0.0005  0.0077  0.0    2     0      0      0     0      0
  0.0080 -0.0002  0.0132  0.0    2     0      0      0     0      0
inflow:
  p1      p2    side (left=1,right=2,up=3,under=4)
outflow:
  p1      p2    side (left=1,right=2,up=3,under=4)
  0.0    0.003    1
  0.0    0.003    2
```

Appendix C

Matlab Files

The file uflux.out, created by the program, has three colomns. Time is written to the first colomn, flux to the second and momentum to the last one.

The following matlab-file, **intensity.m**, is used to calculate the sound pressure level. First, the standard deviation of the momentum is determined and than the formula (2.4) is used.

```
load uflux.out
plot(uflux(:,1),uflux(:,3))
x=uflux(:,3);
t=uflux(:,1);
size=length(t);
y=uflux(25000:size,3);
sd=std(y);
P0=2.0e-5;
SPL=10*log10(sd/((P0)^2))
```

The matlab-file, **spectra.m**, is used to determine the frequency spectrum. This frequency spectrum is made by using the function FFT (Fast Fourier Analysis).

```
load uflux.out
x=uflux(:,2);
size=length(x);
y=uflux(25000:size,2);
Y=fft(y);
Y(1)=0;
fs=1000000;
N=length(Y);
f=[0:N-1]*fs/(N-1);
plot(f,abs(Y))
set(gca,'Xlim',[0 1200],'ylim',[0 60])
```

Remark: fs = 1/(timestep) and can differ in different simulations.

Appendix D

Snapshots

A few plots are given below to get more insight of the movement of the lip near the upper and lower wall. First, a few plots of the model with a pipe before the base of the lip are presented.

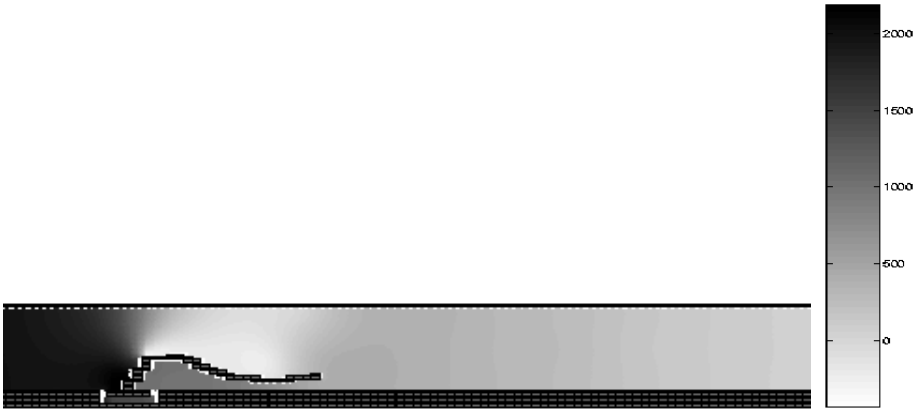

The pressure distribution when the lip almost collides with the lower wall.

The pressure distribution when the lip almost collides with the lower wall.

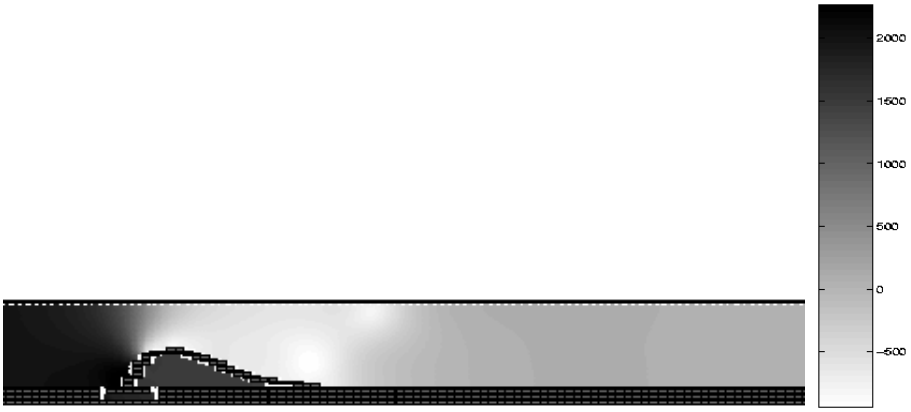

The pressure distribution when the lip collides with the lower wall.

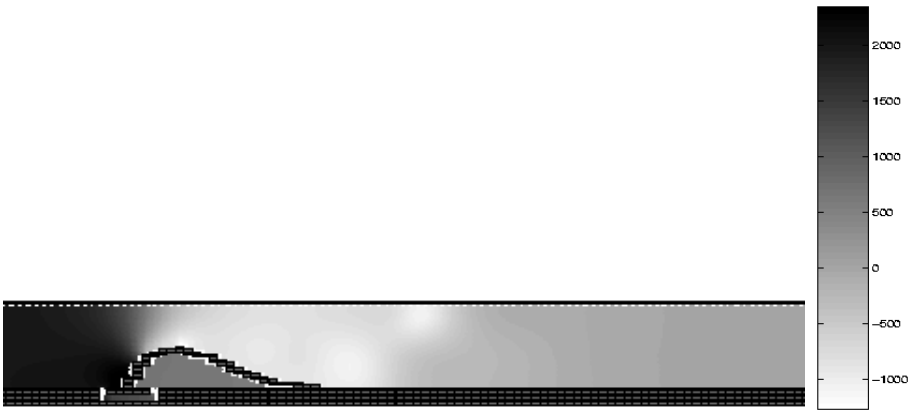

The pressure distribution when the lip is still in contact with the lower wall.

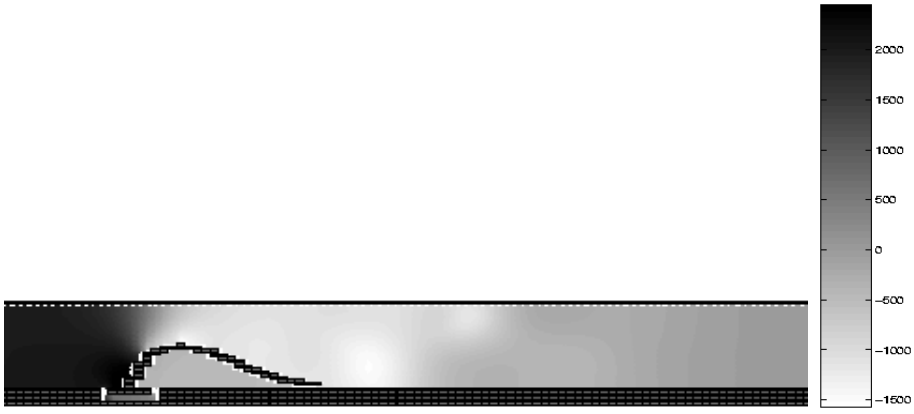

The pressure distribution when the lip goes up again.

The pressure distribution when the lip almost collides with the upper wall.

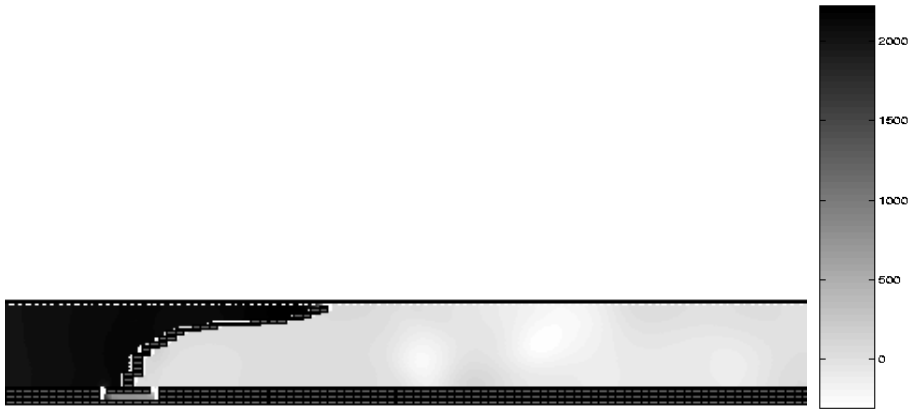

The pressure distribution when the lip almost collides with the upper wall.

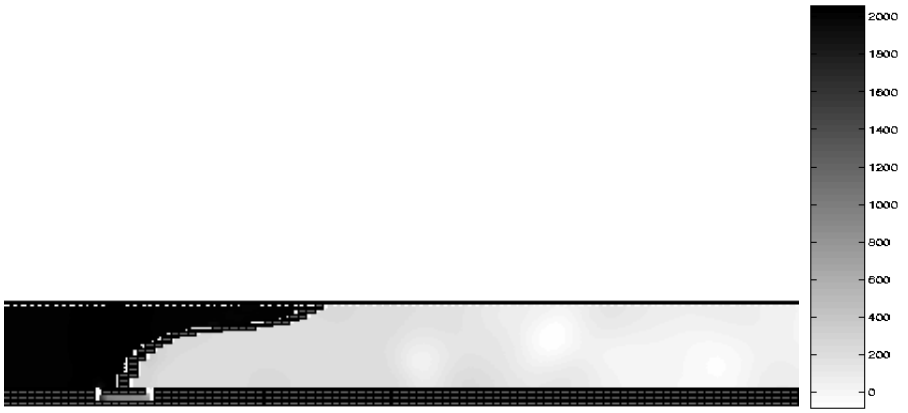

The pressure distribution when the lip collides with the upper wall.

Second, a few plots of the model with a pipe behind the base of the lip are presented.

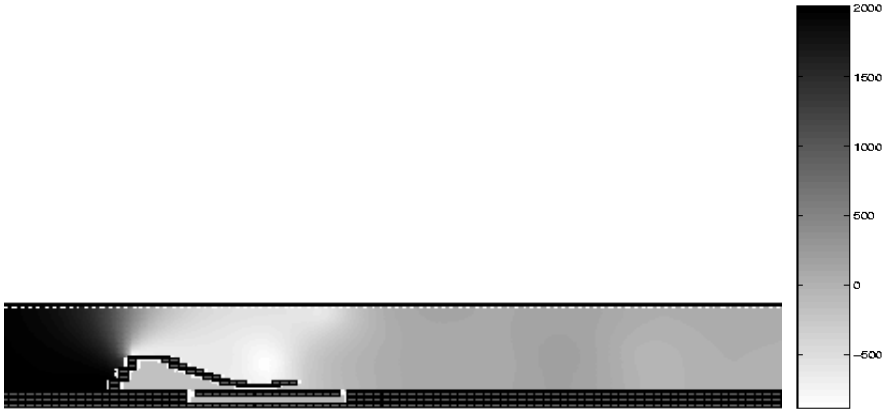

The pressure distribution when the lip almost collides with the lower wall.

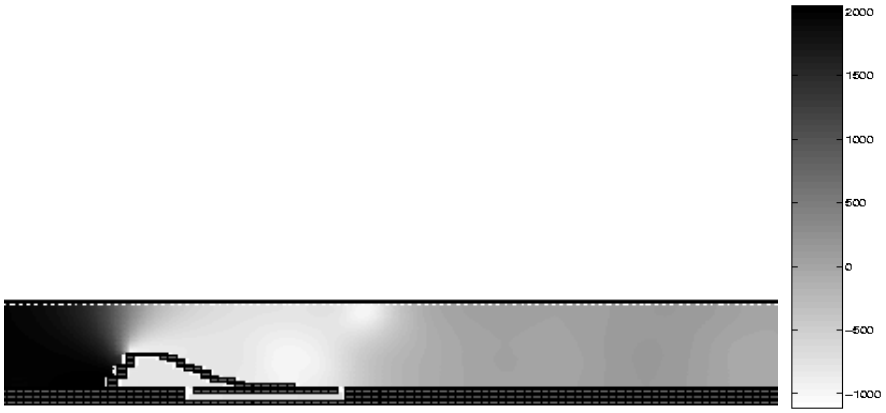

The pressure distribution when the lip collides with the lower wall.

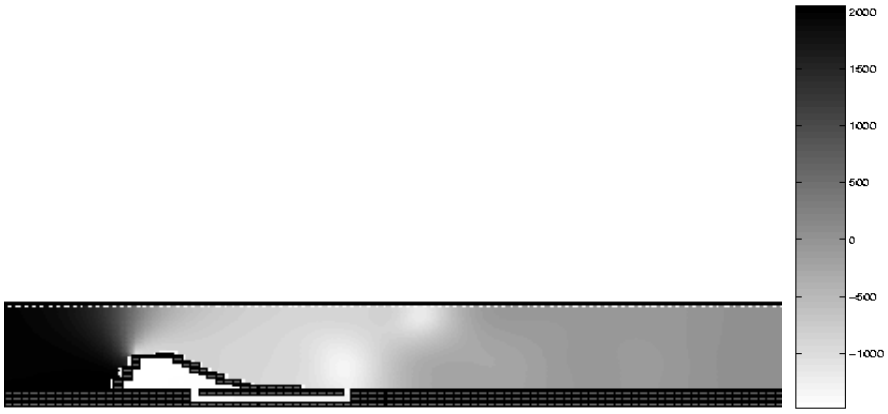

The pressure distribution when the lip is still in contact with the lower wall.

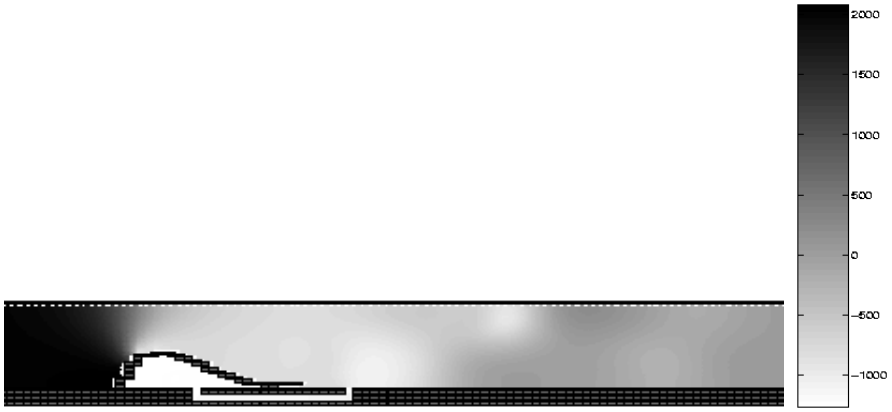

The pressure distribution when the lip is still in contact with the lower wall.

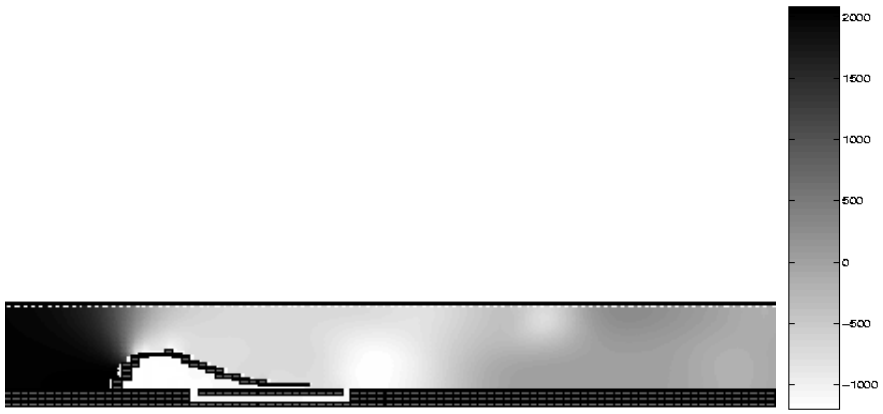

The pressure distribution when the lip goes up again.

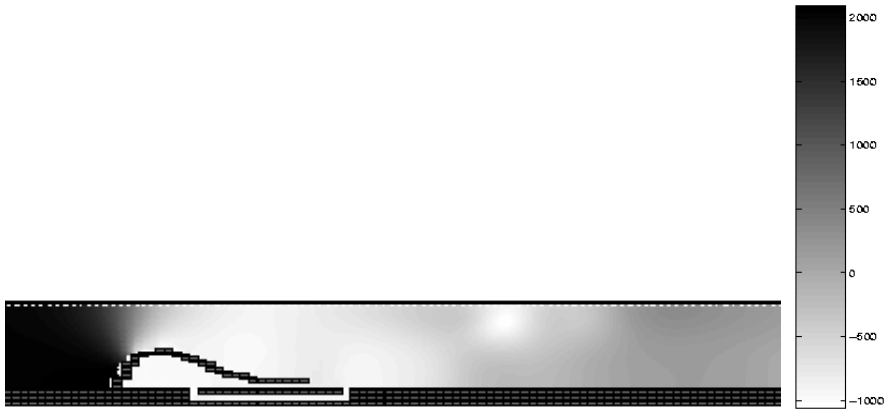

The pressure distribution when the lip goes up again.

The pressure distribution when the lip comes near the upper wall.

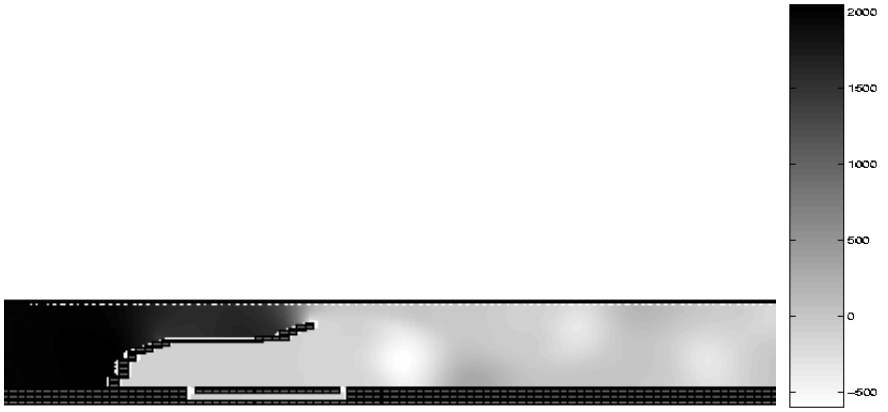

The pressure distribution when the lip comes near the upper wall.

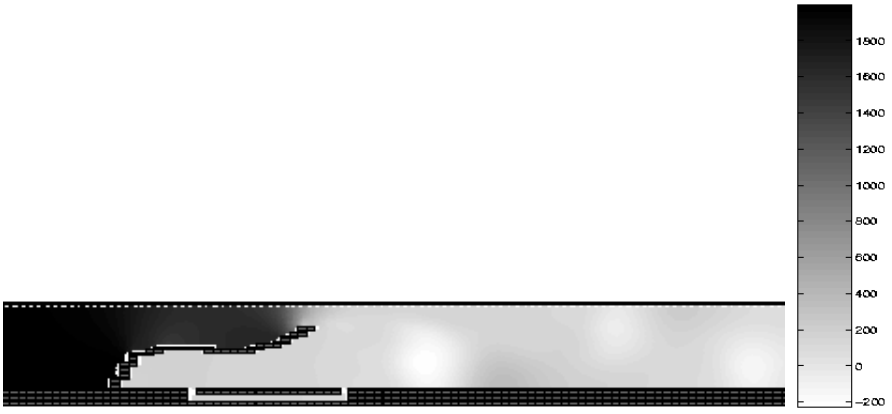

The pressure distribution when the lip goes down again.

Bibliography

[1] Alipour, F., and Titze, I.R. (1988). A finite element simulation of vocal fold vibration, in Proceedings of the Fourteenth Annual Northeast Bio-engineering Conference, Durham, NH, edited by J.R. LaCourse, 186-189.

[2] Alipour-Haghighi, F., and Titze, I.R. (1991). Elastic models of vocal fold tissues, J. Acoust. Soc. Am. 90, 1326-1331.

[3] Alipour, F., and Titze, I.R. (1995). Combined Simulation of Two-dimensional Airflow and Vocal Fold Vibration, NCVS Status and Progress Report 8, 9-14.

[4] Alipour, F., Fan, C., and Scherer, R.C. (1996). A Numerical Simulation of Laryngeal Flow in a Forced-Oscillation Glottal Model, NCVS Status and Progress Report 10, 35-44.

[5] Alipour, F., Berry, D.A., and Titze, I.R. (2000). A finite-element model of vocal fold vibration, J. Acoust. Soc. Am. 108, 3003-3012.

[6] Berg, J.W. van den, Zantema, J.T., and Doornenbal, P. (1957). On the Air Resistance and the Bernoulli Effect of the Human Larynx, J. Acoust. Soc. Am. 29, 626-631.

[7] Berry, D.A., Herzel, H., Titze, I.R., and Krischer, K. (1994). Interpretation of biomechanical simulations of normal and chaotic vocal fold oscillations with empirical eigenfuncties, J. Acoust. Soc. Am. 95, 3595-3604.

[8] Chan, R.W., Titze, I.R. and Titze M.R. (1997). Further studies of phonation threshold pressure in a physical model of the vocal fold mucosa, J. Acoust. Soc. Am. 101, 3722-3727.

[9] Górska, M. (2002). Literature Survey of vocal folds models. University of Groningen.

[10] Guo, C.G., and Scherer, R.C. (1993). Finite element simulation of glottal flow and pressure, J. Acoust. Soc. Am. 94, 688-700.

[11] Hamburg, M.C. (1999). Development of a numerical model of a voice-producing element using the Finite Element Method in combination with Navier-Stokes equations. Master's thesis, Universiteit Twente, October 1999.

[12] Hirano, M. (1974). Morphological structure of the vocal cord as a vibrator and its variations, Folia Phoniatr. 26, 89-94.

[13] Ishizaka, K., and Flanagan, J.L. (1972). Synthesis of voiced sounds from a two-mass model of the vocal cords, Bell Syst. Tech. J. 51, 1233-1267.

[14] Liljencrants, J. (1991). Numerical Simulation of Glottal Flow, in Vocal Fold Physiology: Acoustic, Perceptual and Physiological Aspects of Voice Mechanics, J. Gauffin and B. Hammarberg Eds., San Diego, 99-104.

[15] Pelorson, X., Hirschberg, A., Hassel, R.R. van, and wijnands, A.P.J. (1994). Theoretical and experimental study of quasisteady-flow separation within the glottis during phonation. Application to a modified two-mass model, J. Acoust. Soc. Am. 96, 3416-3431.

[16] Pelorson, X., Hirschberg, A., Wijnands, A.P.J., and Bailliet, H. (1995). Description of the flow through in-vitro models of the glottis during phonation, Acta Acustica 3, 191-202.

[17] Plaats, A. van de (2002). In-vitro measurements of a voice producing element under physiologic acoustic conditions, J. Acoust. Soc. Am., submitted.

[18] Story, B.H., and Titze, I.R. (1995). Voice simulation with a body-cover model of the vocal folds, J. Acoust. Soc. Am. 97, 1249-1260.

[19] Titze, I.R. (1973). The human vocal cords: A mathematical model I, Phonetica 28, 129-170.

[20] Titze, I.R. (1974). The human vocal cords: A mathematical model II, Phonetica 29, 1-21.

[21] Titze, I.R. (1980). Comments on the Myoelastic-Aerodynamic Theory of Phonation, Journal of Speech and Hearing Research 23, 495-510.

[22] Titze, I.R., Baken, R.J., and Herzel, H. (1992). Evidence of chaos in vocal fold vibration, NCVS Status and Progress Rep. 3, 39-63.

[23] Titze, I.R. (1992). Phonation threshold pressure: a missing link in glottal aerodynamics, J. Acoust. Soc. Am. 91, 2926-2935.

[24] Titze, Ingo R. (1994). Principles of Voice Production. Prentice Hall, Englewood Cliffs, New Jersey.

[25] Titze, I.R., Schmidt, S.S. and Titze M.R. (1995). Phonation threshold pressure in a physical model of the vocal fold mucosa, J. Acoust. Soc. Am. 97, 3080-3084.

[26] Torn, M. van der, Mahieu, H.F., and Festen, J.M. (2001). Aero-acoustics of silicone rubber lip reeds for alternative voice production in laryngectomees, J. Acoust. Soc. Am. 110, 2548-2559.

[27] Verdolini-Marston, K., Titze, I.R. and Druker, D.G. (1990). Changes in phonation threshold pressure with induced conditions of hydration, J. Voice 4, 142-151.

[28] Vries, M.P. de (2000). A new voice for the voiceless. Design and in-vitro testing of a voice-producing element. Thesis, University of Groningen, July 2000.

[29] Vries, M.P. de (2002). Personal communication.